Simultaneous Measurements of Mitochondrial NADH and Ca^{2+} during Increased Work in Intact Rat Heart Trabeculae

Rolf Brandes* and Donald M. Bers†

*Novasite Pharmaceuticals, San Diego, California 92121 and †Department of Physiology, Loyola University Chicago, School of Medicine, Maywood, Illinois 60153 USA

ABSTRACT The main goal of this study is to investigate the role of mitochondrial $[Ca^{2+}]$, $[Ca^{2+}]_m$, in the possible up-regulation of the NADH production rate during increased workload. Such up-regulation is necessary to support increased flux through the electron transport chain and increased ATP synthesis rates. Intact cardiac trabeculae were loaded with Rhod-2(AM), and $[Ca^{2+}]_m$ and mitochondrial [NADH] ($[NADH]_m$) were simultaneously measured during increased pacing frequency. It was found that 53% of Rhod-2 was localized in mitochondria. Increased pacing frequency caused a fast, followed by a slow rise of the Rhod-2 signal, which could be attributed to an abrupt increase in resting cytosolic $[Ca^{2+}]$, and a more gradual rise of $[Ca^{2+}]_m$, respectively. When the pacing frequency was increased from 0.25 to 2 Hz, the slow Rhod-2 component and the NADH signal increased by 18 and 11%, respectively. Based on a new calibration method, the 18% increase of the Rhod-2 signal was calculated to correspond to a 43% increase of $[Ca^{2+}]_m$. There was also a close temporal relationship between the rise (time constant ~25 s) and fall (time constant ~65 s) of $[Ca^{2+}]_m$ and $[NADH]_m$ when the pacing frequency was increased and decreased, respectively, suggesting that increased workload and $[Ca^{2+}]_c$ cause increased $[Ca^{2+}]_m$ and consequently up-regulation of the NADH production rate.

SELECTED DEFINITIONS

$[Ca^{2+}]_c(dia, 0.25)$, $[Ca^{2+}]_c(dia, 2)$	=	Cytosolic $[Ca^{2+}]$ in diastole at 0.25 or 2 Hz pacing frequency ($[Ca^{2+}]_c(dia, 0.25)$ measured only with Indo-1, while $[Ca^{2+}]_c(dia, 2)$ measured with Indo-1 or Rhod-2).
$[Ca^{2+}]_m(0.25)$, $[Ca^{2+}]_m(2)$	=	Mitochondrial $[Ca^{2+}]$ at 0.25 or 2 Hz (in diastole) (depends on time-averaged $[Ca^{2+}]_c$; e.g. higher time-averaged $[Ca^{2+}]_c$ with increased frequency).
R2(dia)	=	Total Rhod-2 intensity during diastole (mitochondrial + cytosolic Rhod-2).
$I_{tot}(0.25)$	=	R2(dia) at 0.25 Hz steady-state pacing.
$I_{tot}(2_{init})$	=	Initial R2(dia) following an increase from 0.25 to 2 Hz.
$I_{tot}(2_{SS})$	=	R2(dia) at 2 Hz steady-state pacing.
$\Delta R2_c$	=	Beat-to-beat Rhod-2 transient amplitude (mainly from cytosolic Rhod-2).
$\Delta R2_c(dia)$	=	Amplitude of the fast increase in diastolic Rhod-2 signal with increased frequency ($I_{tot}(2_{init}) - I_{tot}(0.25)$; mainly from cytosolic Rhod-2).
$\Delta R2_m$	=	Amplitude of the slow increase in diastolic Rhod-2 signal with increased frequency ($I_{tot}(2_{SS}) - I_{tot}(2_{init})$; mainly from mitochondrial Rhod-2).
τ_{R2}^{up}	=	Time constant for the slow rise component of the Rhod-2 signal.
τ_{R2}^{down}	=	Time constant for the slow decay component of the Rhod-2 signal.
NADH	=	Semicalibrated $[NADH]_m$ from N_{ratio} (see Eq. 2) or nicotineamid adenine dinucleotide (reduced form).
$[NADH]_m$	=	Mitochondrial [NADH].
NADH MIN	=	Minimum level of NADH following increased work (previously shown to depend on work level).
NADH REC	=	Amount of NADH recovery following prolonged work (hypothesized to depend on $[Ca^{2+}]_m$).
NADH MAX	=	Maximum level of NADH following reduced work ("overshoot"; hypothesized to depend on $[Ca^{2+}]_m$ prior to reducing work.)
τ_{NADH}^{up}	=	Time constant for the slow rise of the NADH signal.
τ_{NADH}^{down}	=	Time constant for the slow decay of the NADH signal.

Submitted December 28, 2000, and accepted for publication April 23, 2002.

Address reprint requests to Rolf Brandes, Dept. of Physiology, Loyola University Chicago, School of Medicine, 2160 South First Ave., Maywood, IL 60153. Tel.: 708-216-6305; Fax: 708-216-6308; E-mail: rbrandes@alumni.ucsd.edu.

0006-3495/02/08/587/18 $2.00

INTRODUCTION

The mechanisms of regulation of oxidative phosphorylation with increased work have recently gained new interest. Evidence has suggested that increased mitochondrial $[Ca^{2+}]$, $[Ca^{2+}]_m$, may, in addition to ADP (Jacobus et al., 1982; Koretsky et al., 1987; Unitt et al., 1989), stimulate the ATP synthesis rate by indirect action on the F_0F_1-ATPase (Wan et al., 1993; Territo et al., 2000). Such downstream regulation of the ATP synthesis rate would result in increased NADH consumption rate, and, consequently, necessitate increased NADH production rates as well. Up-regulation of the NADH production rate has also been hypothesized to be controlled by increased $[Ca^{2+}]_m$, activating pyruvate dehydrogenase (PDH) or tricarboxylic acid cycle dehydrogenases (Hansford, 1991; Crompton, 1990; McCormack et al., 1990). Provided that the activation of the F_0F_1-ATPase and the dehydrogenases occur on different timescales and with different relative magnitudes, slow changes in mitochondrial NADH, $[NADH]_m$, may be observed following increased $[Ca^{2+}]_m$. Increased $[Ca^{2+}]_m$, in turn, is expected following increased (average) cytosolic $[Ca^{2+}]$, $[Ca^{2+}]_c$, such as when the workload is increased by increased pacing frequency (Miyata et al., 1991).

In support of this mechanism, we have previously shown that, in intact cardiac trabeculae, $[NADH]_m$ and average $[Ca^{2+}]_c$ increased when the workload was increased by increased pacing frequency (Brandes and Bers, 1996; Brandes et al., 1998), but $[NADH]_m$ did not increase when the workload was increased by stretching the muscle (no expected increase in $[Ca^{2+}]_c$) (Brandes and Bers, 1997). However, there is little direct evidence that shows that, with increased workload (e.g., by increased pacing frequency), increased $[NADH]_m$ is correlated with increased $[Ca^{2+}]_m$.

The primary goal of this study is therefore to test whether increased pacing frequency causes increased $[Ca^{2+}]_m$ and $[NADH]_m$, and to compare the kinetics of change. To more closely follow the effect of increased $[Ca^{2+}]_m$ on $[NADH]_m$, it is necessary to measure both simultaneously.

Previous studies have used Indo-1 to measure $[Ca^{2+}]_m$ and endogenous fluorescence to measure $[NADH]_m$. A problem with Ca^{2+}-measurements using Indo-1, however, is that its emission spectrum overlaps with that of NADH (~400–500 nm), and changing $[NADH]_m$ would thus affect the Indo-1 signal. In contrast, Rhod-2 fluoresces at a longer wavelength (~590 nm) than Indo-1, making it more suitable for Ca^{2+}-measurements than Indo-1 when $[NADH]_m$ is expected to change. Furthermore, because the Rhod-2 spectrum does not overlap with NADH fluorescence, $[NADH]_m$ measurements may be performed simultaneously with Rhod-2-based Ca^{2+}-measurements (although changes in $[NADH]_m$ can be assessed in the presence of Indo-1 (Brandes et al., 1993a)).

A disadvantage of Rhod-2 versus Indo-1, however, is that the wavelength of the Rhod-2 emission maximum is independent of $[Ca^{2+}]_m$, and Rhod-2 can therefore not be used as a ratiometric dye. It is consequently much more difficult to convert Rhod-2 intensities to explicit $[Ca^{2+}]$ values. A secondary goal of this study was therefore to develop a method whereby quantitative information about $[Ca^{2+}]_m$, or at least relative changes in $[Ca^{2+}]_m$, may be calculated from Rhod-2 fluorescence intensities.

MATERIALS AND METHODS

Trabeculae preparation

Thin band-shaped trabeculae (~200 by 500 μm) were isolated from rat right ventricles as described elsewhere (Brandes and Bers, 1996). Briefly, brown male LBN-F1 rats (370–510 g) were deeply anesthetized and anticoagulated by injecting 65 mg pentobarbital and 1000 U heparin i.p. The hearts were excised and then perfused retrograde before removing the trabeculae. The perfusion solution contained (in mM): NaCl (108), KCl (21), $MgCl_2$ (1.2), $CaCl_2$ (0.5), $NaHCO_3$ (24), Glucose (4), sodium pyruvate (10), insulin (20 units/L) and was equilibrated with a 95% O_2, 5% CO_2 gas mixture to produce pH = 7.40.

After dissection, the muscle was mounted in a muscle chamber (Brandes and Bers, 1996), paced at 0.5 Hz and superfused at 10–15 ml/min with the solution described above except that 6 mM KCl, instead of 21 mM, was used, and initial $[Ca^{2+}]$ = 0.3 mM until force was stable, and then raised to 1.5 mM. Muscle stretch was adjusted to obtain maximum developed force, which was measured during isometric contractions (Backx and Ter Keurs, 1993; Brandes and Bers, 1997). All experiments and procedures were performed at room temperature (~25°C).

Fluorescence instrumentation

Instrumentation described in detail elsewhere (Brandes and Bers, 1996) was modified for simultaneous excitation at two wavelengths (350 and 540 nm) and emission detection at three wavelengths (see Fig. 1): 1) 385 nm: The reference signal for NADH motion correction (Brandes and Bers, 1996) or, alternatively, the lower Indo-1 emission wavelength (Grynkiewicz et al., 1985; Brandes et al., 1994); 2) 456 nm: The NADH emission or, alternatively, the higher Indo-1 emission wavelength (Grynkiewicz et al., 1985; Brandes et al., 1994); and 3) 590 nm: The Rhod-2 emission wavelength.

$[NADH]_m$ measurements

$[NADH]_m$ was assessed using methods described previously (Brandes and Bers, 1996). Briefly, the trabeculae were excited by light at 350 nm, and fluorescence detected at 385 and 456 nm. The use of these tissue light isosbestic wavelengths accounts for possible changes in tissue light absorbance, e.g., due to hypoxia (Brandes et al., 1994). However, as we have demonstrated, the trabeculae were not hypoxic at higher pacing rates (Brandes and Bers, 1996). The fluorescence signal at 456 nm (N456) is predominantly arising from mitochondrial NADH (Eng et al., 1989; Nuutinen, 1984) and motion artifacts. In contrast, the reference signal at 385 nm (due to auto-fluorescence and possibly a small component of back-scattered light; N385) is mainly sensitive to motion artifacts (Brandes and Bers, 1996). We therefore used our previously developed method to eliminate motion artifacts from the NADH fluorescence signal at 456 nm

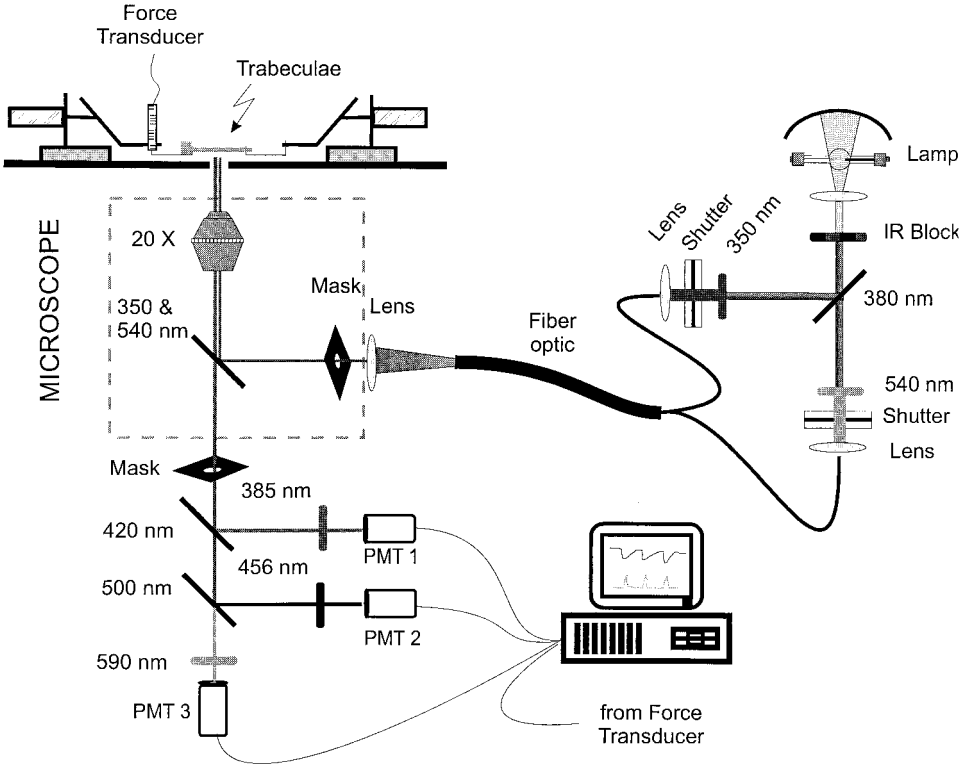

FIGURE 1 Instrumentation used to simultaneously measure NADH (at 385 and 456 nm) and Rhod-2 fluorescence (at 590 nm). The light from a Xenon arc lamp was divided into two paths by a 380-nm dichroic mirror (380 DRLP; Omega Optical, Brattleboro, VT), filtered at 350 nm (20-nm bandwidth) and 540 nm (25-nm bandwidth), respectively (Chroma Technologies, Brattelboro, VT) and recombined using a bifurcated fiber optic cable (Cuda Products Corp, Jacksonville, FL). The dichroic mirror in the inverted microscope (Nikon Diaphot-TMD, Nikon Corp., Melville, NY) was a specially designed mirror that reflected light at 350 and 540 nm, while transmitting light at 375–510 nm and above 560 nm (Chroma Technologies). The transmitted fluorescence passed through two dichroic mirrors (420 and 500 nm; Reynard Corp, San Clemente, CA and Omega Optical) and was subsequently filtered at three wavelengths (385, 456, and 590 nm; bandwidths 22, 10, and 20 nm; Chroma Technologies).

by dividing it with the reference signal (Brandes and Bers, 1996), thus obtaining a fluorescence ratio,

$$N_{\text{ratio}} = \frac{N456}{N385}. \quad (1)$$

Because N385 and N456 gradually decreased during the experimental protocols, and at different rates (Brandes and Bers, 1996; Ashruf et al., 1995), N_{ratio} was normalized relative to its value at a pacing frequency of 0.25 Hz (control value). Occasionally, N_{ratio} slowly changed during the course of a protocol and, in this case, the whole trace was mathematically baseline corrected (by correcting the trace with a second order fitted polynomial so that consecutive N_{ratio} at 0.25 Hz was constant at unity). $[\text{NADH}]_m$ is assessed from N_{ratio} by using a semicalibrated NADH defined such that NADH = 0 when NADH is maximally oxidized, corresponding to $0.49 \cdot N_{\text{ratio}}$ (at 1 Hz steady state) (Brandes and Bers, 1996), and NADH = 1 during baseline conditions (at 0.25 Hz pacing frequency) according to

$$\text{NADH} = \frac{N_{\text{ratio}} - 0.49 \cdot N_{\text{ratio}}(1\ \text{Hz})}{N_{\text{ratio}}(0.25\ \text{Hz}) - 0.49 \cdot N_{\text{ratio}}(1\ \text{Hz})}. \quad (2)$$

This calibration procedure causes the changes in NADH to be up to twice as large as the changes in N_{ratio} (e.g., a 10% change in N_{ratio} would result in a 15–20% change in the calibrated NADH). Changes in NADH will thus be expressed in absolute fractional or percentage units, where NADH at control is unity or 100%. (Note that, because $N_{\text{ratio}}(0\ \text{Hz}) \sim N_{\text{ratio}}(0.25\ \text{Hz})$, calibrated NADH would be similar regardless of whether 0 or 0.25 Hz were used as baseline condition.)

Mitochondrial and cytosolic [Ca^{2+}] measurements in Rhod-2-loaded trabeculae

Trabeculae were loaded with Rhod-2/AM (Molecular Probes, Eugene, OR) to measure cytosolic and mitochondrial [Ca^{2+}] ($[Ca^{2+}]_c$ and $[Ca^{2+}]_m$). Rhod-2/AM was first dissolved with DMSO containing 25% (w/vol.) Pluronic to a concentration of 1 mM, and then diluted 100-fold to a final concentration of 10 μM in Tyrode Buffer containing (in mM) NaCl (140), KCl (6), $MgCl_2$ (1.0), $CaCl_2$ (0.3), Hepes (5), Glucose (10), sodium pyruvate (10), pH = 7.40. Stimulation was ceased, and the trabecula incubated for 50 min at room-temperature (~25°C). The trabecula was then superfused with normal perfusate containing $[Ca^{2+}] = 0.3$ mM for ~5 min or until force relaxed completely, followed by $[Ca^{2+}]_c = 1.5$ mM and pacing at the 0.25 Hz basal frequency for at least 30 min before any measurements. Rhod-2 fluorescence was excited at 540 nm and emission detected at 590 nm (myoglobin isosbestic wavelength with regard to oxygenation; Brandes et al., 1994). At 590 nm, the fluorescence intensity typically increased by 5–10 times after Rhod-2 loading, whereas the intensity at 456 nm (where NADH is detected) only increased by 2–5%.

To assess $[Ca^{2+}]_m$, it is necessary to determine the relative fractions of Rhod-2 that loads into the mitochondria versus the cytosol (by removing

the cytosolic component with digitonin), and to obtain an independent measurement of $[Ca^{2+}]_c$ using a dye that only loads into the cytosol (free salt of Indo-1; see below). Furthermore, because Rhod-2 fluorescence intensity depends both on $[Ca^{2+}]$ and on [Rhod-2], Rhod-2 was saturated with Mn^{2+} to obtain an independent measure of [Rhod-2]. Eqs. A21, A22, and A27 in the Appendix shows the calculation of $[Ca^{2+}]_m$ (at 0.25 and 2 Hz) based on four independent measurements: the total measured Rhod-2 fluorescence (mitochondrial and cytosolic), the total Rhod-2 fluorescence after Mn^{2+} saturation, Indo-1 measured $[Ca^{2+}]_c$, and the relative fraction of cytosolic Rhod-2 dye. Two different methods to determine $[Ca^{2+}]_m$ (2 Hz) are presented to determine whether there is a fast rising component of $[Ca^{2+}]_m$ when the pacing frequency is abruptly increased. If the two methods would produce similar results, it would suggest that $[Ca^{2+}]_m$ does not abruptly increase (see Appendix).

Another method to achieve the same conclusion would be to compare the diastolic values of $[Ca^{2+}]_c$ (2 Hz) immediately following increased pacing frequency, when measured by Rhod-2 versus Indo-1. If the values are similar, it would again suggest that $[Ca^{2+}]_m$ does not abruptly increase when the pacing frequency is abruptly increased (see Appendix). Eq. A30 in the Appendix shows the calculation of $[Ca^{2+}]_c$ (2 Hz), based on the same four independent measurements used to calculate $[Ca^{2+}]_m$.

Cytosolic $[Ca^{2+}]$ measurements in Indo-1-loaded trabeculae

To selectively measure cytosolic $[Ca^{2+}]$, a separate group of trabeculae were iontophoretically loaded with the free acid of Indo-1 (Molecular Probes), as described elsewhere (Maier et al., 1998), because this approach eliminates Indo-1 compartmentalization (Backx and Ter Keurs, 1993). Indo-1 fluorescence was excited at 350 nm, and the emission ratio, I_{ratio} (intensity at 385 vs. 456 nm; I_{385}/I_{456}), was calculated after subtraction of background fluorescence (partly NADH) at each emission wavelength, and accounting for any changes in NADH during the protocol (separately measured) (Brandes et al., 1993a). The intensity of I_{ratio} is related to $[Ca^{2+}]_c$ by (Grynkiewicz et al., 1985)

$$I_{ratio} = \frac{R_{max} \cdot [Ca^{2+}] + R_{min} \cdot K_d \cdot S_{456}}{[Ca^{2+}] + K_d \cdot S_{456}}, \quad (3)$$

or equivalently,

$$[Ca^{2+}]_c = K_d \cdot S_{456} \cdot \frac{I_{ratio} - R_{min}}{R_{max} - I_{ratio}}, \quad (4)$$

where S_{456} is the ratio between the 456-nm Indo-1 emission intensity in the absence of $[Ca^{2+}]_c$ and with saturating $[Ca^{2+}]_c$ (Grynkiewicz et al., 1985). R_{min} and R_{max} are the I_{ratio} values in the absence of $[Ca^{2+}]_c$ and with saturating $[Ca^{2+}]_c$, respectively. The calibration constant S_{456} was determined in a protein solution that mimics intracellular conditions, whereas R_{min} and R_{max} were determined in vivo as described by Brandes et al. (1993b). In contrast, K_d was determined in aqueous solution (see section below).

Determination of Indo-1 and Rhod-2 calibration parameters, K_d, α and β

Because of difficulties in reliably determining K_d in the intracellular milieu (Baker et al., 1994), the K_d of both Indo-1 and Rhod-2 were identically determined in aqueous solutions. The fluorescence intensities were measured as a function of $[Ca^{2+}]$ by successively diluting an EGTA solution with a buffered Ca^{2+}-EGTA solution (Molecular Probes). The mixture contained Rhod-2 or Indo-1 (5.75 and 3 μM, respectively), Ca^{2+} (0–39.8 μM free as calculated from the dilutions), EGTA (10 mM), Mg^{2+} (1.0 mM), K^+ (140 mM) and Hepes (40 mM). Measurements were done at room temperature and adjusting to pH = 7.20. K_d was obtained by nonlinear curve fitting (Microcal Software Inc, Northampton, MA) of the measured intensities of Rhod-2 and Indo-1 ratio versus $[Ca^{2+}]$ using Eqs. A1 and 3, respectively.

As shown in the Appendix, $[Ca^{2+}]$ may be determined from the Rhod-2 fluorescence intensity (I) by using two calibration parameters; $\beta = I_{min}/I_{max}$ and $\alpha = I_{Mn^{2+}}/I_{max}$, where I_{max} is the maximum intensity (with saturating $[Ca^{2+}]$), I_{min} is the minimum intensity (with $[Ca^{2+}] = 0$) and $I_{Mn^{2+}}$ is the intensity with saturating $[Mn^{2+}]$. In contrast to R_{min} and R_{max}, it is difficult to determine α and β in vivo, and they were therefore determined from the same aqueous solution that was used to determine K_d. In fact, β was simply calculated from the fitted values of I_{min} and I_{max} using the K_d measurements. $I_{Mn^{2+}}$, and subsequently α, was determined by adding saturating $[Mn^{2+}] = 250$ μM to the same aqueous solution as that used for the K_d measurements, but without EGTA and minimal Ca^{2+} ($[Ca^{2+}]_0 \sim 5$ μM; typical of de-ionized H_2O as determined with a Ca^{2+} electrode).

Data analysis

A 0.2-Hz low-pass filter was applied to the NADH signal to obtain improved signal-to-noise ratio using software digital filtering (Origin, MicroCal Software Inc.). This filtering also removed the beat-to-beat changes in the NADH signal (Brandes and Bers, 1996). To determine the exponential time constants for changes in the Rhod-2 or NADH signal, nonlinear curve fitting was employed using the exponentially rising or decaying parts of the traces according to

$$Y = Y_0 + A \cdot e^{[(t-t_0)/\tau]} \quad (5)$$

where Y is the R2(dia) or NADH intensity, t_0 is the fitted (extrapolated) start time, Y_0 is the value of Y at $t = t_0$, A is the amplitude of change ($A < 0$ for the rise and $A > 0$ for the decay), and τ is the time constant of the rise or decay of R2(dia) or NADH.

Results were reported as means ± SE. Statistical analysis was performed using Student's t test, and differences were considered significant when $p < 0.05$.

RESULTS

Effects of increased frequency on NADH and Rhod-2 fluorescence

Figure 2 shows an example of a trabecula loaded with Rhod-2/AM, and demonstrates the effects of increased pacing frequency (from 0.25 to 2 Hz) on the NADH fluorescence ratio, the total Rhod-2 fluorescence (cytosolic and mitochondrial Rhod-2), and Force. When the frequency was increased, the diastolic levels of Rhod-2, R2(dia), and Force initially increased abruptly, and $[NADH]_m$ decreased to a minimum (MIN). During continued stimulation at 2 Hz, R2(dia) slowly increased (time constant $\tau_{R2}^{up} \sim 13$ s) and reached a new steady state after ~1 min, at which point the Rhod-2 transient amplitude, $\Delta R2_c$, was similar to that at 0.25 Hz. The slow rise of R2(dia) was accompanied by a similar slow recovery of $[NADH]_m$ (REC) whereas Force was unchanged. When the pacing frequency was returned to 0.25 Hz, R2(dia) and diastolic Force fell abruptly, and $[NADH]_m$ rose to a maximum level (MAX). During continued stimulation at 0.25 Hz, R2(dia) and $[NADH]_m$

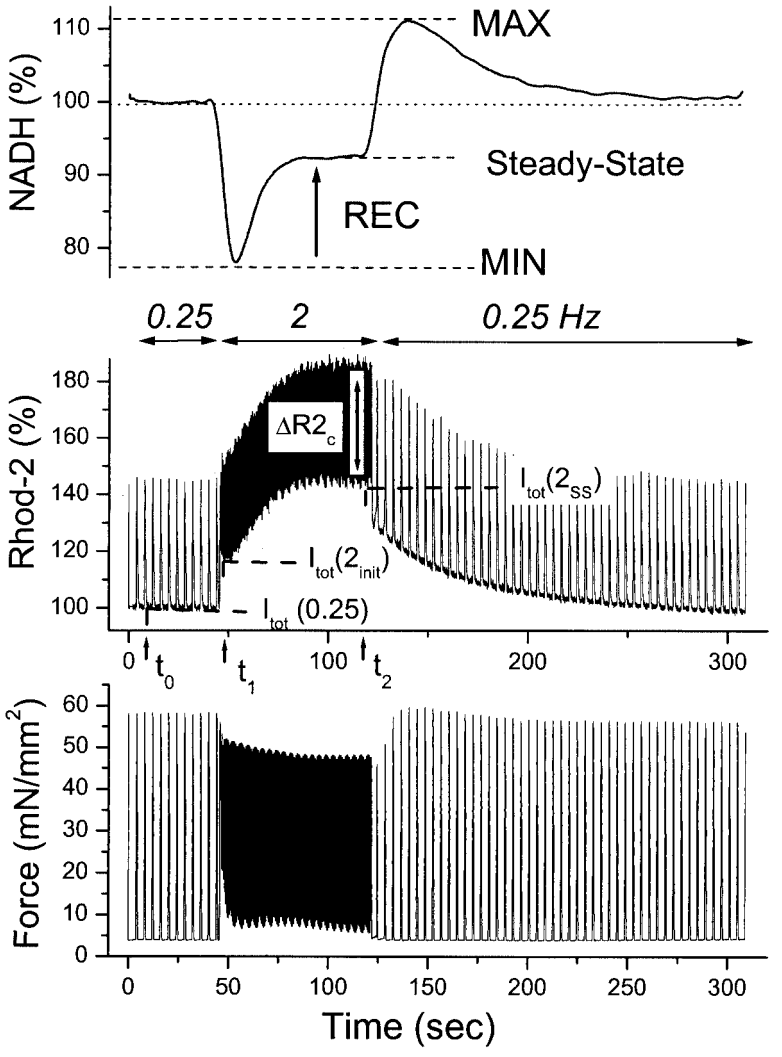

FIGURE 2 Example of changes in NADH fluorescence (*top panel*), Rhod-2 fluorescence (*middle panel*), and Force transients (*bottom panel*) when the pacing frequency is raised from 0.25 to 2 Hz (at t_1 = 46 s) and then back to 0.25 Hz (at t_2 = 122 s). Increased pacing frequency causes a fast rise of Rhod-2 fluorescence ($I_{tot}(0.25)$ to $I_{tot}(2_{init})$), followed by a slower rise ($I_{tot}(2_{init})$ to $I_{tot}(2_{SS})$). See text and Selected Definitions for additional explanation of symbols used.

slowly returned to control values whereas $\Delta R2_c$ was again unchanged.

The changes in $[NADH]_m$ observed here are typical of those that we have reported previously under similar conditions (Brandes and Bers, 1997) and also at more physiological temperatures (37°C) (Brandes and Bers, 1999) and using alternative substrates (Brandes, 1999). The immediate rise of R2(dia) and diastolic Force with increased pacing frequency may be caused by increased diastolic levels of $[Ca^{2+}]_c$ ($[Ca^{2+}]_c$(dia)) affecting cytosolic Rhod-2, whereas the slow rise may be largely caused by slowly increasing levels of $[Ca^{2+}]_m$ affecting mitochondrial Rhod-2. (Because the rise of diastolic Force was relatively small, the rise of $[Ca^{2+}]_c$(dia) may be subthreshold for force development.) Thus, the parallel slow rise of $[NADH]_m$ suggests that it may be caused by an increased NADH production rate which, in turn, may be stimulated by slowly increasing $[Ca^{2+}]_m$.

Because $\Delta R2_c$ and Force transients were similar at 0.25 and 2 Hz, the beat-to-beat Rhod-2 transients may be accounted for by variations in $[Ca^{2+}]_c$. However, some investigators have proposed that small Ca^{2+} transients may also occur in the mitochondria (Sparagna et al., 1995; Buntinas et al., 2001; Trollinger et al., 2000), and such small transients may not be ruled out here based on the results of Fig. 2.

To investigate the hypothesis that the slow rise of the Rhod-2 signal is due to slowly increasing $[Ca^{2+}]_m$, the cytosolic Rhod-2 signal component may possibly be eliminated by displacing Ca^{2+} bound to cytosolic Rhod-2 by the addition of saturating $[Mn^{2+}]$, "Mn^{2+} quenching" (Miyata et al., 1991).

Mn^{2+} quenching of Rhod-2 fluorescence

Other investigators have loaded myocytes with Indo-1/AM and obtained Indo-1 loading in both cytosol and mitochon-

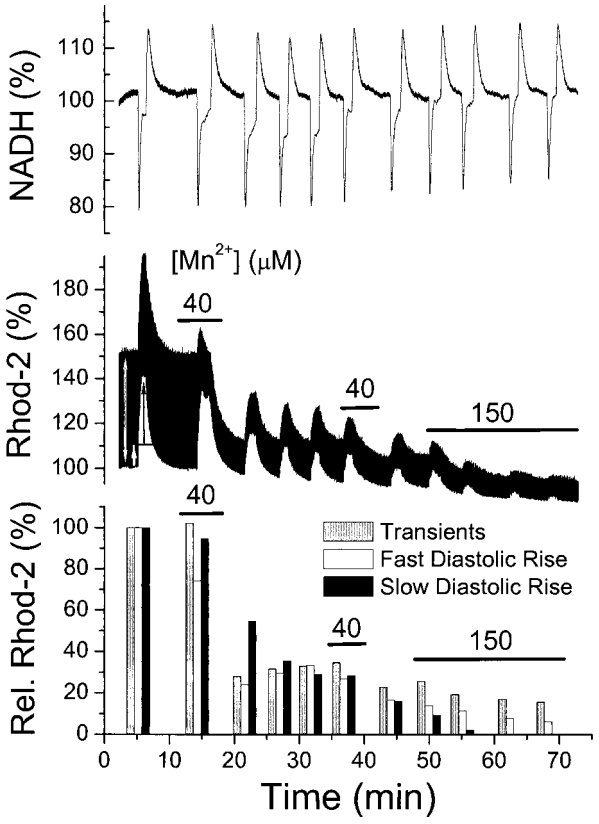

FIGURE 3 Effects of Mn^{2+} quenching of cytosolic and mitochondrial Rhod-2 fluorescence. Application of Mn^{2+} is indicated with a solid bar. Pacing frequency was repeatedly increased and decreased (0.25–2–0.25 Hz) which, before Mn^{2+} quenching (baseline), caused changes in NADH (*top panel*) and Rhod-2 (*middle panel*) similar to those in Fig. 2. In the middle panel, the beat-to-beat Rhod-2 transients are indicated with a gray arrow, the fast Rhod-2 rise with a white arrow, and the slow rise with a black arrow. The bottom panel shows the relative magnitude (versus baseline = 100%) of the transients (*gray bar*), fast rise (*white bar*) and slow rise (*black bar*) as both cytosolic and mitochondrial Rhod-2 were progressively Mn^{2+} quenched.

dria (Spurgeon et al., 1990; Miyata et al., 1991; Schreur et al., 1996). External Mn^{2+} was, in that case, applied to selectively saturate cytosolic Indo-1 but not mitochondrial Indo-1, so that it no longer responded to changes in $[Ca^{2+}]_c$ and only to changes in $[Ca^{2+}]_m$.

To similarly Mn^{2+}-saturate cytosolic Rhod-2 here, trabeculae were carefully titrated with Mn^{2+}-containing perfusate. Figure 3 shows a typical example of an attempt to selectively saturate the cytosolic, but not the mitochondrial, Rhod-2 fluorescence. Before application of Mn^{2+}, the pacing frequency was first increased from 0.25 to 2 Hz, and then returned to 0.25 Hz. The typical changes in NADH and Rhod-2 signal were similar to those shown in Fig. 2. The fast Rhod-2 components, $\Delta R2_c$ (beat-to-beat transients) and $\Delta R2_c$(dia) (fast rising component of R2(dia)) are shown with gray and white arrows, respectively (gray and white bars in the bottom panel). The slower Rhod-2 component, $\Delta R2_m$ (slow rising component of R2(dia)), is shown with a black arrow (and black bar).

The normal perfusion solution was then replaced with one containing 40 μM Mn^{2+} while pacing at 0.25 Hz. The addition of Mn^{2+} did not affect the transients until the frequency was increased to 2 Hz, resulting in a rapid decrease of the transient amplitude. This would suggest accelerated cytosolic Mn^{2+} uptake through the sarcolemma Ca^{2+} channels as the frequency was increased, and subsequent binding of Mn^{2+} to cytosolic Rhod-2. The normal perfusate was then switched back, and the frequency protocol repeated three more times. Figure 3 shows that there was a reduction, both of the Rhod-2 transients (down from 49 to 11%) and of the fast rising component of R2(dia) (down from 16 to 5%). However, the slow rising component of R2(dia) (during stimulation at 2 Hz) was also reduced from 21 to 9%, suggesting mitochondrial Mn^{2+} uptake and subsequent partial quenching of mitochondrial Rhod-2.

Additional Mn^{2+} was then added to saturate both the cytosolic and mitochondrial Rhod-2. Because no slow increase of R2(dia) was apparent when the frequency was increased to 2 Hz (at 62 and 68 min), it is likely that mitochondrial Rhod-2 was completely saturated with Mn^{2+}. This level of Mn^{2+} did not seem to interfere with the Ca^{2+}-dependent stimulation of NADH production or contraction, because the NADH recovery and Force transients (not shown) were similar regardless of $[Mn^{2+}]$. Thus, the $[Mn^{2+}]$ used here did not interfere with Ca^{2+}-dependent activation of the mitochondrial dehydrogenases or Force generation.

Although the mitochondrial Rhod-2 was completely Mn^{2+} saturated, residual Rhod-2 transients were sometimes observed. These may be due to three factors. 1) Motion (and noise) artifacts: because Rhod-2 is not a ratiometric dye, its detected intensity is sensitive to motion artifacts (Brandes et al., 1992), which would manifest itself as a beat-to-beat response. 2) Cytosolic Ca^{2+} transients: even though large amounts of Mn^{2+} were added, it may not have been enough to completely saturate cytosolic Rhod-2 at maximum $[Ca^{2+}]_c$ (peak of the transient). Attempting to eliminate the transients by addition of higher $[Mn^{2+}]_0$ resulted in reduced contraction (because of interference with the Ca^{2+}-channels). 3) Mitochondrial Ca^{2+} transients: it is unlikely that any mitochondrial Ca^{2+} transients would be large enough to displace Mn^{2+} at the peak (i.e., as for cytosolic Rhod-2), because Mn^{2+} was able to eliminate the work-dependent Ca^{2+} increase, and this was larger than the transients (e.g., see Fig. 3 at 20 min immediately following partial Mn^{2+} quenching of cytosolic Rhod-2). However, we cannot exclude the unlikely possibility that there may be two fractions of mitochondrial Rhod-2: one that senses the work-dependent rise of $[Ca^{2+}]_m$ and is quenched by Mn^{2+}, and another fraction that senses any mitochondrial Ca^{2+} transients, but is not quenched.

In contrast to Mn^2-saturated Indo-1, where the fluorescence intensity is very weak (see cuvette experiments below), the intensity of Mn^2-saturated Rhod-2 was still significant because R2(dia) only decreased by 22% in this example and, on average, decreased by 25 ± 3% (n = 5), i.e., $I_{Mn^{2+}} = 0.75 \cdot I_{tot}(0.25)$ or $I^*_{tot}(0.25) = 1.33$ (Eq. A12). Note that this is an upper-limit estimate. The real Mn^{2+}-dependent decrease may be slightly less if some dye leaked out of the cytosol during the protocol. (A Rhod-2 leak from the mitochondria to the cytosol would, of course, not matter, because Rhod-2 would remain quenched by cytosolic Mn^{2+}).

Verification of mitochondrial Rhod-2 loading

The pacing protocol above suggested that Rhod-2 was compartmentalized into (at least) two compartments; cytosol and mitochondria. To further investigate this, three different protocols were evaluated.

Fraction of mitochondrial Rhod-2

To determine the relative fractions of mitochondrial versus cytosolic Rhod-2, the cytosolic fraction was selectively washed out by permeabilizing the sarcolemma membrane with digitonin (20 μM) while leaving the mitochondrial membrane intact (Spurgeon et al., 1990; Leyssens et al., 1996). Mn^{2+} (200 μM) was first added to saturate Rhod-2 and thus obtain a Ca^{2+}-independent measure of the dye concentration.

Figure 4 shows that digitonin addition initially caused a transient rise of the Rhod-2 signal. This can be explained by a rise in $[Ca^{2+}]_c$ from the resting level of $[Ca^{2+}]_c \sim 167$ nM to $[Ca^{2+}]_o \sim 5$ μM (typical of de-ionized water) when the sarcolemma membrane was permeabilized. After perfusion for 8 min, the Rhod-2 signal fell, and eventually reached a new lower level, consistent with removal of cytosolic Rhod-2.

To verify that the remaining Mn^{2+}-saturated Rhod-2 is localized in mitochondria, mitochondrial dye was washed out by also permeabilizing the mitochondrial membrane using Triton-X (1%) (Leyssens et al., 1996). Again, the transient rise of the Rhod-2 signal indicates permeabilization of the mitochondrial membrane. Any remaining background fluorescence was measured with regular perfusion solution, and was insensitive to trifluoromethoxyphenylhyrazone (FCCP) or Ca^{2+} (1.5 mM) and therefore only contributes with a small constant intensity (mainly due to instrumental factors). After subtraction of this background component, it was found that 45% of the Rhod-2 signal came from the cytosol, and 55% from the mitochondria. On average, 47 ± 7% (n = 4) of the Rhod-2 dye was found to be localized in the cytosol.

Sometimes digitonin permeabilization caused a slow decline of the fluorescence intensity after the initial relatively fast drop, and a steady state was not always reached. This approach may therefore be somewhat less reliable in the intact trabeculae versus isolated cells when accurate quantification of the cytosolic versus mitochondrial Rhod-2 fractions is needed. Nevertheless, a 10% error in the determination of the loading fraction only causes a 6% error in the calculation of $[Ca^{2+}]_m$ (per Eq. A20).

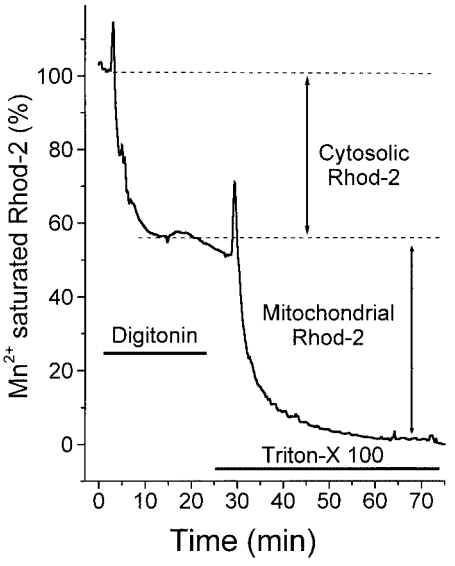

FIGURE 4 Determination of cytosolic versus mitochondrial Rhod-2 loading. Digitonin (*solid bar*) is expected to release cytosolic Rhod-2 while Triton-X 100 (*solid bar*) is expected to release the remainder, most likely in the mitochondria. Following Digitonin application, the Rhod-2 fluorescence dropped relatively fast and reached a new lower value after 8–10 min. However, this drop was sometimes followed by a slower decrease, and the level at 12 min was therefore used in all experiments.

Mitochondrial uncoupling

To demonstrate that a fraction of the Rhod-2 signal is sensitive to changes in mitochondrial $[Ca^{2+}]$, $[Ca^{2+}]_m$ was selectively altered by eliminating the mitochondrial electrochemical gradient using an uncoupler (FCCP) (Di Lisa et al., 1993). Figure 5 illustrates the protocol used. After perfusion with normal perfusate (containing 140 mM Na^+), it was replaced with a low Na^+-containing solution ($[Na^+]$ = 37 mM and $[Li^+]$ = 103 mM). The low extracellular $[Na^+]$ causes reduced cytosolic $[Na^+]$ and increased $[Ca^{2+}]$ (via Na^+/Ca^{2+} exchange), and, consequently, a rise of mitochondrial $[Ca^{2+}]$ (Miyata et al., 1991). Consistent with this, Fig. 5 shows that low $[Na^+]$ caused increased Rhod-2 fluorescence, which peaked at 128% above control level, and increased resting Force.

During prolonged perfusion with low $[Na^+]$, both Rhod-2 and resting Force decreased and reached new steady-state levels. This can be explained by extrusion of cytosolic Ca^{2+} by the sarcolemma Ca^{2+}-pump (ATPase) and some recov-

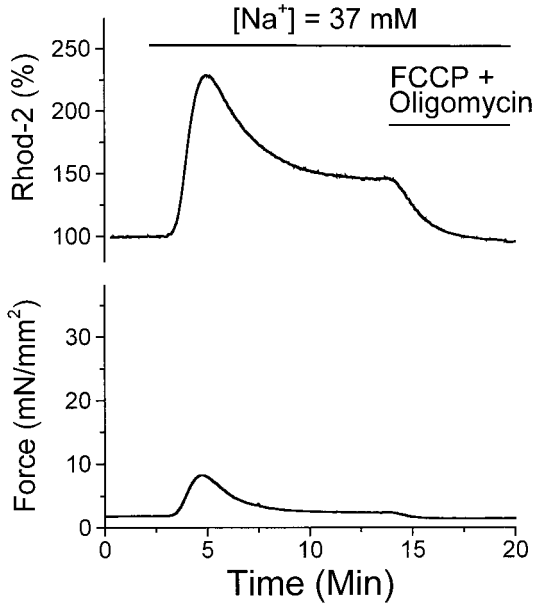

FIGURE 5 Validation of mitochondrial Rhod-2 loading by manipulating $[Ca^{2+}]_m$. $[Ca^{2+}]_m$ (and $[Ca^{2+}]_c$] was first raised by switching to low Na^+ perfusion (*solid bar*), and mitochondrial Ca^{2+} was subsequently released by dissipating the mitochondrial electrochemical gradient by applying a mitochondrial uncoupler, FCCP. Oligomycin (ATPase inhibitor) was simultaneously applied to prevent complete ATP hydrolysis. The resulting changes in Rhod-2 fluorescence were mirrored by changes in resting Force (*bottom panel*) and are further explained in the text. Note, however, the small absolute change in resting Force, which was ~20% of the typical twitch amplitude.

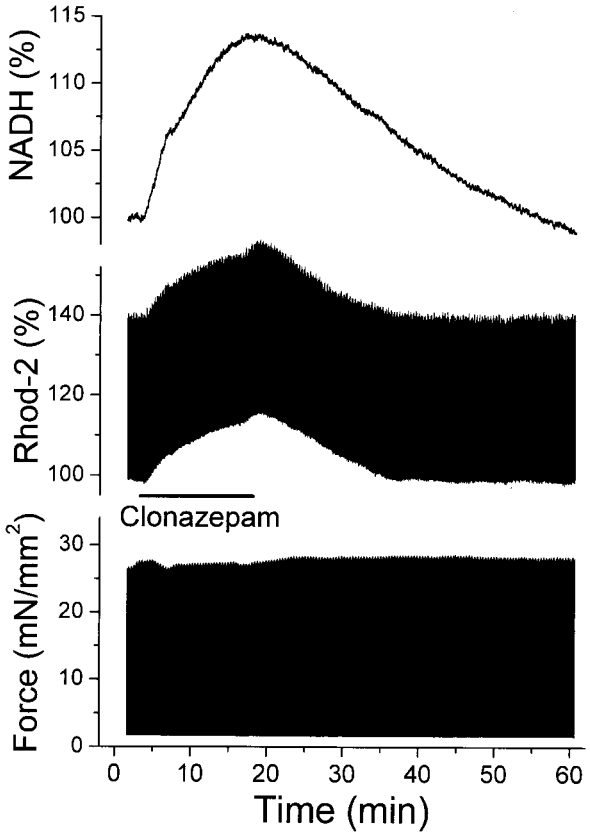

FIGURE 6 Validation of mitochondrial Rhod-2 loading by manipulating $[Ca^{2+}]_m$ by blocking the mitochondrial Na^+/Ca^{2+} exchanger with clonazepam (100 μM, *solid bar*). Application of clonazepam caused increased Rhod-2 fluorescence (*middle panel*) and increased NADH fluorescence (*top panel*), while Force was unaffected (*bottom panel*).

ery of the ability of Na^+/Ca^{2+} exchange to extrude Ca^{2+} as intracellular $[Na^+]$ declines. Although resting Force was only slightly above control level at this new steady state, the Rhod-2 fluorescence was still elevated by ~46% relative to control level. This would suggest that $[Ca^{2+}]_m > [Ca^{2+}]_c$ because half of the Rhod-2 is cytosolic and the other half mitochondrial. Significantly elevated $[Ca^{2+}]_m$ relative to control may be due to inhibition of the mitochondrial Na^+/Ca^{2+} exchanger by the lower-than-normal cytosolic $[Na^+]$.

When FCCP (2 μM) and Oligomycin (5 μg/ml) are added, the elevated $[Ca^{2+}]_m$ is expected to fall, while $[Ca^{2+}]_c$ is still kept low because of $[Ca^{2+}]_c$ regulation by the sarcolemmal Ca^{2+} pump and Na^+/Ca^{2+} exchanger. Thus, total Rhod-2 fluorescence intensity is expected to fall as was observed in Fig. 5. In parallel, Force fell, and this is probably due to inhibition of ATP synthesis as we have also shown previously (Brandes and Bers, 1996). (Note that, because Oligomycin was added here, the reverse mode of the ATP synthase was inhibited, and this prevented complete depletion of ATP and associated rigor development).

Inhibition of mitochondrial Na/Ca^{2+} exchanger

An alternative method of increasing $[Ca^{2+}]_m$ is to use clonazepam, an inhibitor of the mitochondrial Na/Ca^{2+} exchanger (Cox and Matlib, 1993; Griffiths et al., 1997b). A problem with the use of this compound is that it absorbs light (peaking at 310 nm in aqueous solution), and thus reduces the emission intensity of NADH (which is exited at 350 nm). Light absorbance scans also showed that the absorbance spectrum is right-shifted toward longer wavelengths in hydrophobic solution such as DMSO, resulting in increased light absorbance at 350 nm. Consequently, the fluorescence decreases as clonazepam accumulates intracellularly. Fortunately, in our case, the NADH sensitive ratio I_{456}/I_{385}), compensates for the changes in light absorbance in these experiments.

Figure 6 shows an example of the effects of clonazepam on the total Rhod-2 signal, NADH and Force while pacing at 0.5 Hz. When clonazepam was added, the baseline Rhod-2 signal increased by 15%, and this was accompanied by a rise in NADH by 13% without any effects on Force. Removal of clonazepam caused both the Rhod-2 signal and NADH to decrease back to control values. These results suggest that clonezepam causes increased $[Ca^{2+}]_m$, which, in turn, increases the NADH production rate and $[NADH]_m$.

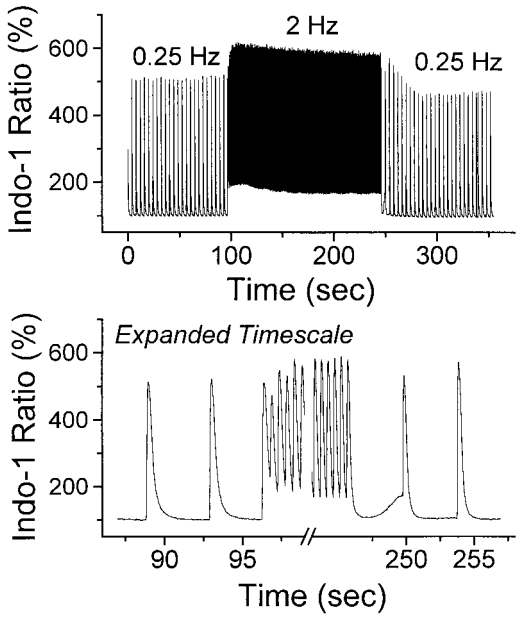

FIGURE 7 Effect of pacing frequency (0.25–2–0.25 Hz) on cytosolic [Ca^{2+}] and Indo-1. Top and bottom panels (expanded time scale of top panel) shows that increased frequency caused an immediate rise of Indo-1 fluorescence that was not followed by a slower rise (in contrast to Rhod-2 fluorescence; see Fig. 2).

Effects of increased frequency on $[Ca^{2+}]_c$ using Indo-1

To verify that the fast diastolic component of the Rhod-2 signal (see Fig. 2) may be caused by alteration in diastolic $[Ca^{2+}]_c$, a separate group of trabeculae were loaded with Indo-1 (free acid). Because Indo-1 was loaded iontophoretically, the Indo-1 ratio is expected to only be related to cytosolic $[Ca^{2+}]_c$ (Backx and Ter Keurs, 1993).

Figure 7 shows a typical example of the effects of increased followed by decreased pacing frequency (0.25–2–0.25 Hz) on the Indo-1 ratio. Within less than one second, a change in pacing frequency caused a corresponding change in diastolic levels of $[Ca^{2+}]_c$. In contrast to the Rhod-2 signal (see Fig. 2), there was no slow rise in the Indo-1 signal after the pacing frequency was increased. These results suggest that the slow Rhod-2 component is not due to changes in $[Ca^{2+}]_c$, and probably reflects changes in $[Ca^{2+}]_m$.

To calibrate these signals, the Indo-1 calibration parameters R_{min} and R_{max} were determined in the trabeculae (Brandes et al., 1993b). In contrast, K_d = 247 nM was determined in aqueous solution (cuvette) as described in the Methods section. Cuvette studies also demonstrated that addition of saturating Mn^{2+} caused complete quenching of Indo-1 fluorescence (not shown), in contrast to Rhod-2 fluorescence (see below). At a pacing frequency of 0.25 Hz, $[Ca^{2+}]_c$(dia, 0.25) = 167 ± 27 nM, and at 2 Hz, $[Ca^{2+}]_c$(dia, 2) = 305 ± 37 nM (n = 6) (Eq. 4). Thus, increasing pacing frequency from 0.25 to 2 Hz caused $[Ca^{2+}]_c$(dia) to increase by 138 ± 30 nM (83%; paired comparison).

Estimation of $[Ca^{2+}]_m$ at 0.25 Hz using Rhod-2

To estimate $[Ca^{2+}]_m$, the Rhod-2 calibration constants K_d, $\alpha = I_{Mn^{2+}}/I_{max}$ and $\beta = I_{min}/I_{max}$ were first determined in a cuvette. Figure 8 *A* shows emission spectra of Rhod-2 with excess EGTA (I_{min}), saturating $[Ca^{2+}]$ (I_{max}) or saturating $[Mn^{2+}]$ ($I_{Mn^{2+}}$) and for $[Ca^{2+}]$ = 150 and 225 nM. As can be seen, the Mn^{2+}-saturated intensity, $I_{Mn^{2+}}$, is similar to the intensity obtained with $[Ca^{2+}]$ somewhere between 150 and 225 nM. Figure 8 *B* shows a nonlinear fit of the Rhod-2 intensities to Eq. A1 to calculate K_d = 1344 nM, I_{min} and I_{max}. The fitted values of I_{min} and I_{max} were then used, together with $I_{Mn^{2+}}$, to calculate β = 0.02274, and α = 0.1477. (Note that these values and Eq. A17 may be used to confirm that $[Ca^{2+}]$ = 197 nM would have the same intensity as $I_{Mn^{2+}}$ by using $I_c = I_{Mn^{2+}}$ (i.e., $I_c^* = 1$), $f_c = 1$ and the fitted Rhod-2 K_d).

To calculate $[Ca^{2+}]_m$(0.25), each trabecula was saturated with Mn^{2+} to determine I_{tot}^*(0.25) and then permeabilized with digitonin and TritonX-100 to determine f_c (as shown above). These data were then used together with the separately determined average value of $[Ca^{2+}]_c$(dia, 0.25) = 167 nM to calculate $[Ca^{2+}]_m$(0.25) = 440 ± 28 nM (n = 5) (Eq. A21).

Because α and β are calculated as ratios of Rhod-2 intensities, they are independent of [Rhod-2] (and instrumental factors), and only depend on the dye characteristics. However, it should be cautioned that they were determined in an aqueous solution, and α and β may therefore differ in the intracellular milieu. For example, we have previously shown that a protein such as albumin (0.3 mg/ml) shifts the Indo-1 isosbestic wavelength from 450 to 427 nm, similar to the in vivo value (Brandes et al., 1993b). We therefore examined the effects of albumin (0.3 mg/ml) on I_{min}, I_{max}, and $I_{Mn^{2+}}$ but did not find any significant differences. Nevertheless, careful studies using various intracellular proteins (Baker et al., 1994) may reveal a larger effect on I_{min}, I_{max}, and $I_{Mn^{2+}}$ and thus on α and β, and this may consequently change the absolute values of $[Ca^{2+}]_m$ reported here. Similarly, the in vivo K_d for Indo-1 and Rhod-2 would most likely be different from the solution values found here and would change the absolute value of $[Ca^{2+}]_m$(0.25). If the K_d for Indo-1 and Rhod-2 would change with similar relative amounts (e.g., both with a factor of ~2) due to dye–protein interactions, calculations using Eqs. 4 and A20 showed that $[Ca^{2+}]_m$(0.25) would simply scale proportionally.

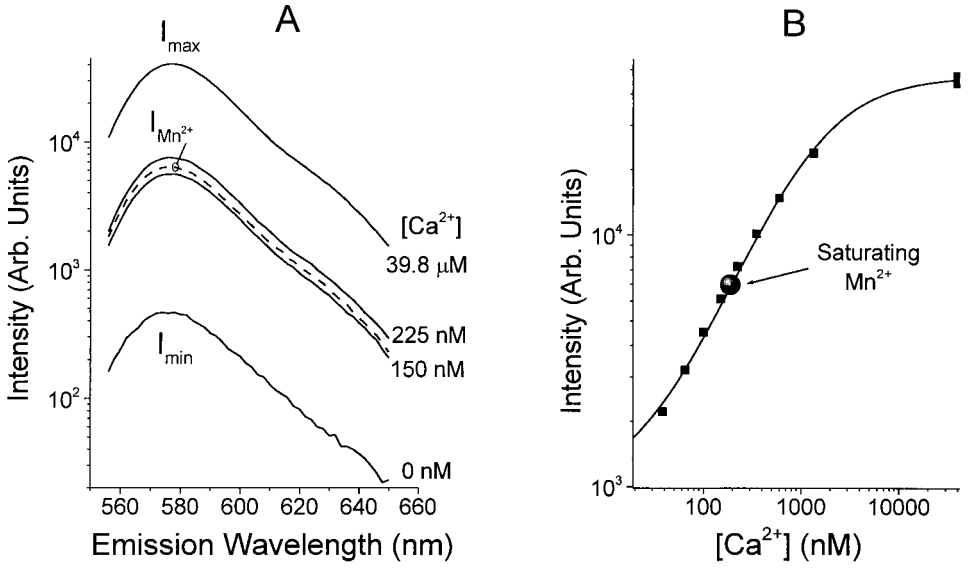

FIGURE 8 Solution (cuvette) calibration of Rhod-2 dye. (*A*) Selected emission spectra using $[Ca^{2+}] = 0$, 150, 225 nM and saturating concentration (39.8 μM). The spectra with saturating Mn^{2+} ($I_{Mn^{2+}}$, *dashed line*) falls between $[Ca^{2+}] = 150$ and 225 nM. (*B*) Nonlinear fit of the emission values at 578 nm (peak) using Eq. A1 to obtain fitted values for I_{min}, I_{max}, and K_d. The values of I_{min}, I_{max}, and $I_{Mn^{2+}}$ were subsequently used to calculate α and β. For comparison, the intensity $I_{Mn^{2+}}$, is also shown on the fitted curve.

Effects of increased frequency on $[NADH]_m$, $[Ca^{2+}]_m$, and $[Ca^{2+}]_c$ using Rhod-2

Figure 9 shows the parameters used to characterize the Rhod-2 and NADH signals. The slow changes in Rhod-2 and NADH observed when the frequency was increased from 0.25 to 2 Hz are characterized by the slow increase in R2(dia), $\Delta R2_m$ (related to $\Delta[Ca^{2+}]_m$), and by the slow increase in $[NADH]_m$ (ΔNADH), and the time constants of the slow rise of R2(dia), τ_{R2}^{up} (related to the rise time of $[Ca^{2+}]_m$), and of NADH, τ_{NADH}^{up} (NADH recovery-time constant). Two additional time constants related to $[Ca^{2+}]_m$ and NADH characterize the return to control after the pacing frequency was lowered back to 0.25 Hz; τ_{R2}^{down} and τ_{NADH}^{down}. Figure 9 additionally shows the amplitude of the fast beat-to-beat Rhod-2 transients (at 0.25 and 2 Hz), $\Delta R2_c$ and the fast rise of R2(dia), $\Delta R2_c$(dia).

Figure 10 shows pooled data from 11 trabeculae. When the pacing frequency was increased from 0.25 to 2 Hz, R2(dia) increased; $\Delta R2_m = 18 \pm 2\%$ with a time constant $\tau_{R2}^{up} = 23 \pm 5$ s. After the initial decrease, $[NADH]_m$ recovered in parallel with increasing R2(dia), ΔNADH = $11 \pm 2\%$ with a time constant $\tau_{NADH}^{up} = 28 \pm 8$ s. Thus, NADH increased by approximately the same relative amount as Rhod-2, and with a similar time constant (the slightly longer time constant for NADH versus R2(dia) was not significantly different). During the final phase, after the frequency was reduced back to 0.25 Hz, both R2(dia) and NADH relaxed with similar time constants; $\tau_{R2}^{down} = 53 \pm 6$ s and $\tau_{NADH}^{down} = 78 \pm 12$ s (the slightly longer time constant for NADH was again not significantly different).

To calculate $[Ca^{2+}]_m(2)$ from Rhod-2 intensities, two different methods were used.

METHOD 1. In the first method, $I_{tot}^*(2)$ was approximated by using the average value of $I_{tot}^*(0.25) = 1.33$ (from a separate set of trabeculae; see Eq. A31) and combined with the average values of $f_c = 0.47$ and $[Ca^{2+}]_c(2) = 305$ nM, obtained from Indo-1 measurements, and substituted into Eq. A22 to obtain $[Ca^{2+}]_m(2) = 582 \pm 57$ nM ($n = 11$).

METHOD 2. In the second method, the rise of $\Delta R2_m$ was analyzed by using the linear combination of intensities (See Eq. A27) to calculate $[Ca^{2+}]_m(2) = 676 \pm 45$ nM (no significant difference versus Method 1).

To investigate the possibility that $\Delta R2_c$(dia) is partially affected by fast mitochondrial Ca^{2+} kinetics (in addition to changes in $[Ca^{2+}]_c$), the result of using the two approaches may be compared. As shown in the Appendix, Method 2 assumed that $[Ca^{2+}]_m$ did not initially increase when the pacing frequency was increased. If this assumption is incorrect, $[Ca^{2+}]_m(2)$ would be underestimated, e.g., $[Ca^{2+}]_m(2)$ would be lower when using Method 2 than when using Method 1. Because this was not found, the assumption is probably correct.

In addition to using Rhod-2 measurements to calculate $[Ca^{2+}]_m(2)$, it may also be used to calculate $[Ca^{2+}]_c$(dia, 2) (using Indo-1 determined $[Ca^{2+}]_c$(dia, 0.25); Eq. A30). With this approach, $[Ca^{2+}]_c$(dia, 2) = 232 ± 15 nM, which is not larger than when Indo-1 alone was used to determine $[Ca^{2+}]_c$(dia, 2) = 305 ± 37 nM (i.e., no significant difference in $[Ca^{2+}]_c$(dia, 2) using Indo-1 versus Rhod-2). Thus, as also explained in the Appendix, Rhod-2 determination of

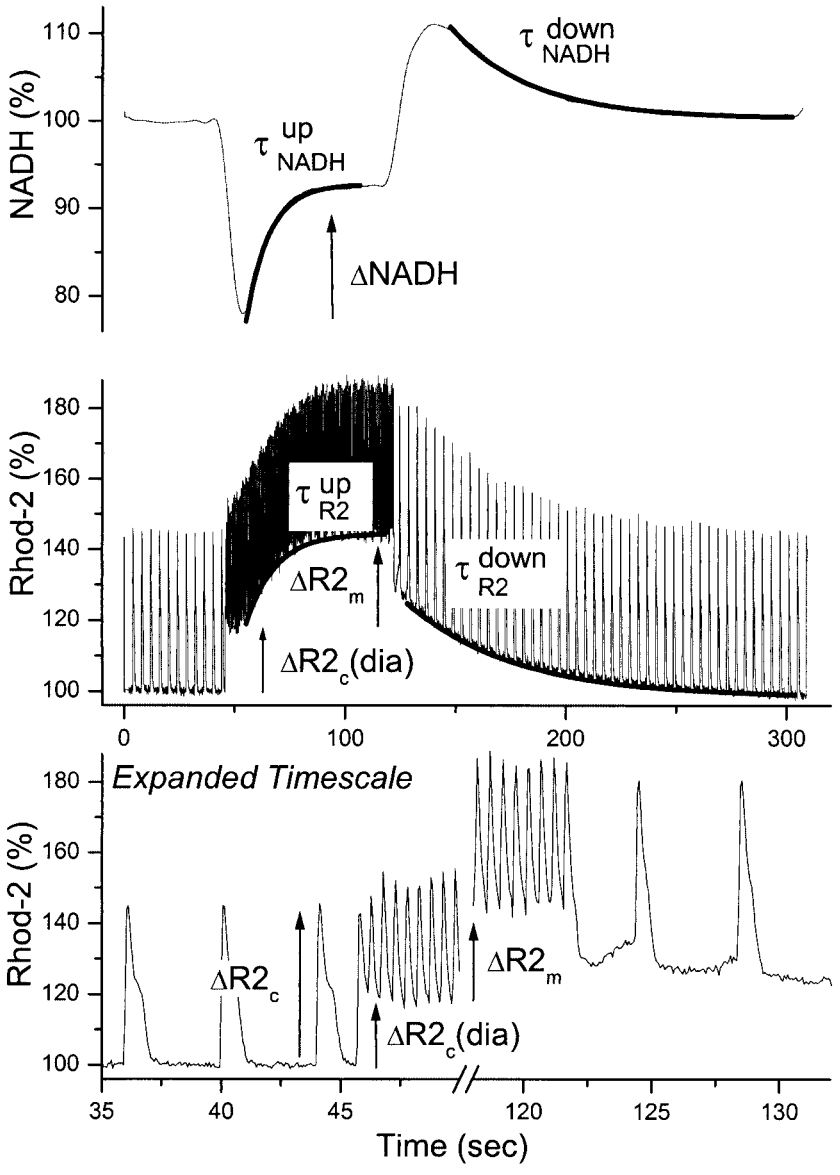

FIGURE 9 Parameters used to characterize frequency-dependent changes in NADH (*top panel*, ΔNADH, τ^{up}_{NADH}, and τ^{down}_{NADH}) and Rhod-2 (*middle* and *bottom panels*, $\Delta R2_c$, $\Delta R2_c$(dia), $\Delta R2_m$, τ^{up}_{R2}, and τ^{down}_{R2}). The bottom panel shows the same data as in the middle panel but on an expanded time scale. As discussed in the text, $\Delta R2_c$(dia) is mainly related to a fast rise in $[Ca^{2+}]_c$, while $\Delta R2_m$ is related to a slow rise in $[Ca^{2+}]_m$. The frequency was transiently increased from 0.25 to 2 Hz at t = 45–122 s.

$[Ca^{2+}]_c$(dia, 2) does not overestimate the "true" $[Ca^{2+}]_c$(dia, 2) (as determined by Indo-1) and the assumption of initially unchanged $[Ca^{2+}]_m$ is also confirmed by this type of measurements.

Both these results (Methods 1 versus 2, and Rhod-2 versus Indo-1 determination of $[Ca^{2+}]_c$(dia, 2); see Table 1). suggest that, as the pacing frequency is suddenly increased, the fast rise of the diastolic Rhod-2 signal, $\Delta R2_c$(dia), can be accounted for by the rise of $[Ca^{2+}]_c$ alone, without an additional component due to a fast rise of $[Ca^{2+}]_m$. However, it is possible that a concurrent small rise of $[Ca^{2+}]_m$ slightly contributes to the fast $\Delta R2_c$(dia) rise, but it may not be detectable with the methods used here. Nevertheless, for the purpose of this study, the main focus is the relationship between the slow recovery of NADH and increased $[Ca^{2+}]_m$ and any possible component of fast mitochondrial Ca^{2+} kinetics is therefore not important here.

The average value of $[Ca^{2+}]_m(2)$ using Methods 1 and 2 is 629 nM, and this is 43% larger than $[Ca^{2+}]_m(0.25)$ = 440 nM. As discussed above, a problem with absolute quantification is that the calculated $[Ca^{2+}]_c$ and $[Ca^{2+}]_m$ are proportional to K_d, and its in vivo value is difficult to determine. However, a change in Rhod-2 K_d alone or a similar proportional change in both Rhod-2 and Indo-1 K_d would not alter the relative increase of $[Ca^{2+}]_m$ (43%) when the pacing frequency is increased (see Eqs. 4 and A20). Furthermore, this relative increase is quite insensitive to an unproportional change in Indo-1 K_d versus Rhod-2 K_d. For example, if Indo-1 K_d is doubled from its aqueous value, while Rhod-2 K_d is unchanged, the rela-

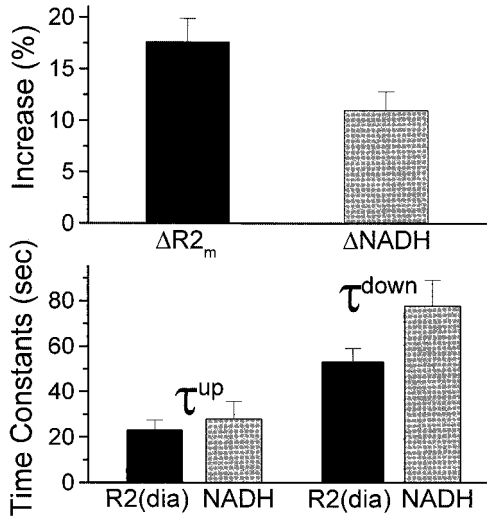

FIGURE 10 Relationships between changes in NADH and R2(dia) (related to $[Ca^{2+}]_m$). The top panel shows that increased NADH, ΔNADH, was related to increased R2(dia), $\Delta R2_m$. The bottom panel shows that the time constants for the rise and fall of NADH and R2(dia) were similar (no significant difference, although the observed longer time constants for NADH is consistent with a causal relation).

tive increase in $[Ca^{2+}]_m$ would only change by 9% (from 43 to 52%).

DISCUSSION

We have previously shown that increased work, due to increased pacing frequency, caused a slow recovery of $[NADH]_m$ (Brandes and Bers, 1996). The primary goal of this study was to determine whether this slow recovery could be explained by slowly increasing mitochondrial $[Ca^{2+}]$ (stimulating the NADH production rate and therefore increased $[NADH]_m$). Our current results are consistent with this hypothesis: as the pacing frequency was increased, both $[Ca^{2+}]_m$ and $[NADH]_m$ increased with a time constant of ~25 s. Conversely, when the pacing frequency was lowered, both $[Ca^{2+}]_m$ and $[NADH]_m$ decreased with a time constant of ~65 s.

A secondary goal was to estimate the change in $[Ca^{2+}]_m$ when the pacing frequency was increased. It was shown that calibration of $[Ca^{2+}]_m$ was feasible using Rhod-2, without the need to obtain I_{max}, if, instead, the Mn^{2+}-saturated Rhod-2 intensity was obtained together with separately determined $[Ca^{2+}]_c$ and the cytosolic versus mitochondrial Rhod-2 loading fraction.

Mn^{2+} quenching of Rhod-2 fluorescence

As shown here, the quenching of mitochondrial Rhod-2 occurred so fast that it was not possible to selectively exclude cytosolic Rhod-2 from mitochondrial Rhod-2 at any time after Mn^{2+} application. This appears to be in contrast to the studies using Indo-1 in hearts (Schreur et al., 1996; Griffiths et al., 1997a), where cytosolic Indo-1 was significantly quenched before mitochondrial Indo-1, but in accordance with studies using Fura-2 (Haworth and Redon, 1998). To explain the different results in the different studies, it is possible that there were differences in mitochondrial Mn^{2+} uptake rates (e.g., due to differing membrane potential) or that there were differences in the kinetics of Mn^{2+} binding to mitochondrial versus cytosolic dye.

Verification of mitochondrial Rhod-2 loading

Using Digitonin permeabilization, Miyata et al. (1991) showed that, in cardiac myocytes, loaded at 23°C, 40% of Indo-1 was localized in the mitochondria. Furthermore, because Mn^{2+} completely quenches Indo-1 (but not Rhod-2) fluorescence, Miyata et al. (1991) and Schreuer et al. (1996) used Mn^{2+} to determine the residual mitochondrial fluorescence, and similarly found that 47% and 53%, respectively, of Indo-1 was loaded in the mitochondria. These similar results, 53% for Rhod-2 here and 40–53% for Indo-1, are in contrast to the results of del Nido et al. (1998) and Trollinger et al. (2000), who found 0 and 100%, re-

TABLE 1 Comparison of $[Ca^{2+}]_c$ and $[Ca^{2+}]_m$ values from Indo-1 and Rhod-2 measurements

Frequency (Hz)	Indo-1 $[Ca^{2+}]_c$(dia) (nM)	Rhod-2 $[Ca^{2+}]_c$(dia) (nM)	Rhod-2 $[Ca^{2+}]_m$ (nM)
0.25	167 ± 26 (Eq. 4)	—	440 ± 28 (Eq. A21)
2	305 ± 37* (Eq. 4)	232 ± 15* (Eq. A30)	582 ± 57†; Method 1 (Eq. A22) (Using $[Ca^{2+}]_c(2)$ from Indo-1)
			676 ± 45†; Method 2 (Eq. A27) (Assuming : I^*_m (0.25) = I^*_m (2init))
0.25 → 2 Hz	$\Delta[Ca^{2+}]_c$ = 138 (+83%)		$\Delta[Ca^{2+}]_m$ = 142 (+32%) or 236 (+54%)

K_d-values used for the calculations were obtained from solution studies; 247 nM for Indo-1 and 1344 nM for Rhod-2 (see text).
*No significant difference between using Indo-1 versus Rhod-2 to determine $[Ca^{2+}]_c$(dia, 2).
†No significant difference between using Rhod-2 Method 1 versus Method 2 to determine $[Ca^{2+}]_m(2)$.

spectively, of Rhod-2 localized in the mitochondria. This large discrepancy may be due to various loading conditions and methods of evaluating mitochondrial dye loading.

Previous studies have shown that inhibition of the mitochondrial Na^+/Ca^{2+} exchanger by clonazepam caused increased $[Ca^{2+}]_m$ (as measured by Indo-1) and $[NADH]_m$ (Griffiths et al., 1997b), consistent with the results obtained here. Furthermore, we also found that the rise of Rhod-2 and $[NADH]_m$, was similar when using clonazepam or the frequency jump: Rhod-2 = 15 vs. 18% and NADH = 13 vs. 11%.

Estimation of $[Ca^{2+}]_m$ at 0.25 Hz using Rhod-2

Other authors have assessed $[Ca^{2+}]_m$ by using Mn^{2+} to selectively quench cytosolic Indo-1 (Schreur et al., 1996; Griffiths et al., 1997a). A complication with this approach, as shown here, is that some Mn^{2+} is likely to enter the mitochondria (Hunter et al., 1980, 1981; Haworth and Redon, 1998) and thus also quench mitochondrial Indo-1. However, provided that Mn^{2+} quenches the fluorescence at both emission wavelengths identically, the fluorescence ratio should be constant. This would require, among other things, that the background fluorescence is measured prior to dye loading and then remains constant for accurate subtraction. Because the background fluorescence is, in general, not constant (Brandes and Bers, 1996; Ashruf et al., 1995), it is possible that the ratio would change after Mn^{2+} quenching, giving incorrect estimates of $[Ca^{2+}]_m$.

In contrast to Indo-1, Rhod-2 is not a ratiometric dye, and Mn^{2+} quenching can thus not be used when Mn^{2+} enters the mitochondria. Furthermore, Mn^{2+} does not completely quench the Rhod-2 fluorescence and this complicates matters further. To solve this problem here, the fraction of mitochondrial Rhod-2 loading combined with the total Rhod-2 intensity after Mn^{2+} saturation was determined to calculate $[Ca^{2+}]_m$ = 440 ± 28 nM at 0.25 Hz. This is higher than the value obtained in isolated myocytes at 0.3 Hz; $[Ca^{2+}]_m$ = 200 nM (Griffiths et al., 1997a), and may be attributed to physiological differences (e.g., isometrically contracting trabeculae versus isolated myocytes). Alternatively, the dye calibration may be incorrect due to a $[Ca^{2+}]_m$-insensitive component of the dye(s) (e.g., incomplete de-esterification or compartmentalization into lysosomes (Trollinger et al., 2000)), or due to differences in the K_d used to calculate $[Ca^{2+}]_m$.

It is well established that K_d is strongly dependent on dye–protein interactions and on dye–ion interactions (Baker et al., 1994; Hove-Madsen and Bers, 1992), and the dye interactions in the intracellular milieu is not known. For example, the solution value for Rhod-2 has been reported to be K_d = 570 nM (in the absence of Mg^{2+}; Molecular Probes), but K_d = 1344 nM was found here (with Mg^{2+}). Thus, if K_d = 570 nM was used instead, $[Ca^{2+}]_m(0.25)$ = 187 nM and $[Ca^{2+}]_m(2)$ = 287 nM, and this is more similar to the values found in isolated myocytes (Griffiths et al., 1997a).

Effects of increased frequency on $[NADH]_m$, $[Ca^{2+}]_m$, and $[Ca^{2+}]_c$ using Rhod-2

When the pacing frequency was increased from 0.25 to 2 Hz, there was an immediate fall of $[NADH]_m$ that we have previously shown to be Ca^{2+}-independent (Brandes and Bers, 1997), and may be due to increased [ADP] (Unitt et al., 1989), stimulating the oxidative phosphorylation rate and thereby the fall of $[NADH]_m$. There has also been some evidence suggesting that, in addition, there is a Ca^{2+}-dependent stimulation of oxidative phosphorylation by indirectly activating the F_0F_1–ATPase (Wan et al., 1993; Territo et al., 2000).

With continued pacing at the higher rate, $[Ca^{2+}]_m$ and $[NADH]_m$ rose slowly with a time constant of ~25 s. This rise of $[Ca^{2+}]_m$ is most likely mediated via Ca^{2+} uptake via the uniporter (Gunter et al., 1994), and suggests that the rise of $[Ca^{2+}]_m$ stimulates mitochondrial enzymes (PDH or the TCA cycle enzymes; α-ketoglutarate or NADH-linked isocitrate dehydrogenase) to increase the NADH production rate (Hansford, 1991) and thereby $[NADH]_m$. The rise of $[Ca^{2+}]_m$, with a time constant of ~25 s, is similar to that observed elsewhere (Miyata et al., 1991; Bassani et al., 1993) and predicted by simulations (Crompton, 1990). In these simulations, the mitochondria effectively act as a low-pass filter, reducing the matrix-transient amplitude versus the cytosol. If the cytosolic amplitude is increased, both the mitochondrial Ca^{2+} transients and steady-state $[Ca^{2+}]_m$ increases. Similarly, an increase of the pacing frequency would slowly (~25 s) increase $[Ca^{2+}]_m$. Because we simultaneously measured changes in cytosolic and mitochondrial $[Ca^{2+}]$, we were not able to separately measure the relative magnitudes of cytosolic versus mitochondrial Ca^{2+} transients.

The experimental protocol used here to increase average $[Ca^{2+}]_c$, and consequently $[Ca^{2+}]_m$, by increased pacing frequency, differs from other studies using isolated mitochondria where $[Ca^{2+}]_m$ was increased by rapid-step increases of extra-mitochondrial Ca^{2+} (Buntinas et al., 2001; Territo et al., 2001). In the study by Territo et al., addition of 535 nM Ca^{2+} to a suspension of Ca^{2+}-depleted mitochondria resulted in a very rapid rise of $[Ca^{2+}]_m$ (<100 ms) and a slower rise of $[NADH]_m$ ($\tau \sim 6$ s). The large sudden step increase of extra-mitochondrial $[Ca^{2+}]$ apparently results in a much faster phase of mitochondrial Ca^{2+} uptake than observed here when the pacing frequency, and consequently time-averaged $[Ca^{2+}]_c$ was increased. The observed rise of $[NADH]_m$ following stimulation depends on the NADH production rate (e.g., Ca^{2+} stimulation of the dehydrogenases) being larger than the NADH consumption rate (e.g., Ca^{2+} and ADP stimulation of the F_0F_1–ATPase). Thus, if the NADH production rate increases faster than the consumption rate, $[NADH]_m$ will rise faster than when the NADH consumption rate also increases fast. In the case of increased work (e.g., the trabeculae studied

here), the fast increase of the NADH consumption rate is expected to cause a slower rise of $[NADH]_m$ than stimulation without increased work (e.g., isolated mitochondria). Indeed, as shown in Fig. 2, the large NADH consumption rate with increased pacing frequency even caused $[NADH]_m$ to fall before it recovered. The difference in the Ca^{2+} protocols and the difference in $[NADH]_m$ consumption rates could explain the differences between the kinetics of $[Ca^{2+}]_m$ and $[NADH]_m$ in the two different types of studies.

Although increased $[Ca^{2+}]_m$ has previously been observed following increased pacing rates (Miyata et al., 1991), this has generally not been associated with increased $[NADH]_m$ in freely contracting myocytes (White and Wittenberg, 1995) unless norepinephrine was added (Griffiths et al., 1997b, 1998). The reason for the limited NADH response in isolated myocytes versus the isometrically contracting trabeculae used here is not clear, but may partly depend on substrate used (pyruvate was added to the glucose here) and also on workload and associated ATP consumption rates, which could change the balance between NADH production and consumption, and thus $[NADH]_m$.

When the frequency was lowered back to control, the decreased rate of oxidative phosphorylation resulted in excess NADH production due to continued stimulation of the mitochondrial dehydrogenases by mitochondrial Ca^{2+}. As $[Ca^{2+}]_m$ slowly decreased, presumably by slow mitochondrial Na^+/Ca^{2+} exchange (Crompton, 1990; Gunter et al., 1994), both $[Ca^{2+}]_m$ and $[NADH]_m$ returned to control values with similar time constants of ~65 s. The slower fall versus rise of $[Ca^{2+}]_m$ when the frequency was increased and decreased, is consistent with the idea that the Na^+/Ca^{2+} exchanger operates at a slower rate than the uniporter (Crompton, 1990) and data suggesting net mitochondrial Ca^{2+} efflux in intact cells with a time constant of ~40 s (Bassani et al., 1993).

The ~43% increase of $[Ca^{2+}]_m$ when the pacing frequency was increased from 0.25 to 2 Hz in the trabeculae is close to the value found in isolated mycotes when the frequency was increased from 0.2 to 2 Hz; 83 nM to ~125 nM, or ~50% (Miyata et al., 1991). Interestingly, the $K_{0.5}$ for pyruvate dehydrogenase activation is ~650 nM (Di Lisa et al., 1993) allowing for efficient regulation of its activity for the range of $[Ca^{2+}]_m$ observed here; 440 to 676 nM. In contrast, the change in $[Ca^{2+}]_m$ reported in myocytes; 83 to 125 nM is expected to produce much smaller alterations in activity of this enzyme.

CONCLUSIONS

We have shown that, when increased work is associated with increased average $[Ca^{2+}]_c$, such as increased pacing frequency, this causes slowly increasing $[Ca^{2+}]_m$ and this is closely related to an equivalently slow rise of $[NADH]_m$. Thus, Ca^{2+} may act as a control signal to increase the flux of reducing equivalents needed to support an increased rate of oxidative phosphorylation and ATP synthesis. In parallel, ADP and $[Ca^{2+}]_c$ may act as control signals to increase the rate of ATP synthesis by modulating the activity of the F_0F_1–ATPase.

APPENDIX

Calculation of $[Ca^{2+}]_m$ provided that $[Ca^{2+}]_c$ is known

The Rhod-2 fluorescence intensity, I, is related to $[Ca^{2+}]$ according to (Grynkiewicz et al., 1985)

$$I = \frac{I_{max} \cdot [Ca^{2+}] + I_{min} \cdot K_d}{[Ca^{2+}] + K_d}, \tag{A1}$$

where K_d is the Rhod-2 dissociation constant for Ca^{2+}, and I_{max} and I_{min} are Rhod-2 calibration parameters; I_{max} is the maximum intensity (with saturating $[Ca^{2+}]$) and I_{min} is the minimum intensity (with $[Ca^{2+}] = 0$).

A serious problem with Rhod-2 in vivo is that it may partition into (at least) two compartments, e.g., cytosol and mitochondria, and the total measured intensity, I_{tot}, is then given by

$$I_{tot} = I_c + I_m. \tag{A2}$$

I_c and I_m are the intensities of Rhod-2 localized in the cytosol and mitochondria respectively, given by

$$I_c = f_c \frac{I_{max} \cdot [Ca^{2+}]_c + I_{min} \cdot K_d}{[Ca^{2+}]_c + K_d}, \tag{A3}$$

$$I_m = f_m \frac{I_{max} \cdot [Ca^{2+}]_m + I_{min} \cdot K_d}{[Ca^{2+}]_m + K_d}, \tag{A4}$$

where $[Ca^{2+}]_c$ and $[Ca^{2+}]_m$ are the cytosolic and mitochondrial $[Ca^{2+}]$, and f_c and f_m are the fractional concentrations of Rhod-2 in the cytosol and mitochondria, i.e.,

$$f_c = \frac{[Rhod2]_c}{[Rhod2]_c + [Rhod2]_m}, \tag{A5}$$

$$f_m = 1 - f_c = \frac{[Rhod2]_m}{[Rhod2]_c + [Rhod2]_m}. \tag{A6}$$

In Eqs. A3 and A4, it was assumed that the dye characteristics were similar in the cytosol and mitochondria, i.e., K_d, I_{max}, and I_{min} were identical in both compartments (Spurgeon et al., 1990).

Cytosolic and mitochondrial $[Ca^{2+}]$ are equivalently related to the Rhod-2 intensities by

$$[Ca^{2+}]_c = K_d \frac{I_c - I_{min} \cdot f_c}{I_{max} \cdot f_c - I_c}, \tag{A7}$$

$$[Ca^{2+}]_m = K_d \frac{I_m - I_{min} \cdot (1 - f_c)}{I_{max} \cdot (1 - f_c) - I_m}. \tag{A8}$$

To solve for $[Ca^{2+}]_m$, $I_m = I_{tot} - I_c$ (per Eq. A2) is substituted into Eq. A8,

$$[Ca^{2+}]_m = K_d \frac{(I_{tot} - I_c) - I_{min} \cdot (1 - f_c)}{I_{max} \cdot (1 - f_c) - (I_{tot} - I_c)}. \tag{A9}$$

Eq. A9 demonstrates that $[Ca^{2+}]_m$ can be calculated from the measured total intensity, I_{tot}, provided that both $[Ca^{2+}]_c$ and f_c (which is needed to calculate I_c) are separately determined.

A problem with the approach described above, however, is that the measured intensities depend not only on [Ca^{2+}], but also on I_{max} and I_{min}, which in turn depend on [Rhod-2]. To eliminate the dependency on [Rhod-2], it is necessary to independently assess the concentration. Because Mn^{2+} binds much more strongly to Rhod-2 than does Ca^{2+} (lower K_d), Rhod-2 may be saturated with Mn^{2+} to obtain an intensity, $I_{Mn^{2+}}$, which depends on [Rhod-2] but not on [Ca^{2+}]. From this, a Ca^{2+}-dependent ratio intensity, I^*, which depends on $[Ca^{2+}]_c$ and $[Ca^{2+}]_m$, but not on [Rhod-2] and instrumental factors, is calculated:

$$I_c^* = I_c/I_{Mn^{2+}}, \tag{A10}$$

$$I_m^* = I_m/I_{Mn^{2+}}, \tag{A11}$$

$$I_{tot}^* = I_c^* + I_m^* = I_{tot}/I_{Mn^{2+}}. \tag{A12}$$

Similarly, two new calibration constants α and β, that are independent of [Rhod-2] (and instrument characteristics), but depend on the intrinsic properties of the Rhod-2 dye, may be defined as

$$\alpha = I_{Mn^{2+}}/I_{max}, \tag{A13}$$

$$\beta = I_{min}/I_{max}, \tag{A14}$$

where I_{max}, I_{min}, and K_d is determined from cuvette studies of Rhod-2 using Ca^{2+}-EGTA buffers (Molecular Probes; see Methods). Thus, intracellular [Ca^{2+}] may conveniently be determined using Rhod-2 by simply determining I_{tot}^* in vivo and combining this with the in vitro cuvette-determined constants, α and β as shown below.

Substituting Eqs. A10, A13, and A14 into Eq. A3, and also Eqs. A11, A13, and A14 into Eq. A4 gives

$$I_c^* = f_c \frac{[Ca^{2+}]_c + \beta \cdot K_d}{\alpha \cdot (K_d + [Ca^{2+}]_c)}, \tag{A15}$$

$$I_m^* = f_m \frac{[Ca^{2+}]_m + \beta \cdot K_d}{\alpha \cdot (K_d + [Ca^{2+}]_m)}. \tag{A16}$$

Solving for $[Ca^{2+}]_c$ and $[Ca^{2+}]_m$, respectively, gives

$$[Ca^{2+}]_c = K_d \cdot \frac{f_c \cdot \beta - \alpha \cdot I_c^*}{\alpha \cdot I_c^* - f_c}, \tag{A17}$$

$$[Ca^{2+}]_m = K_d \cdot \frac{(1 - f_c) \cdot \beta - \alpha \cdot I_m^*}{\alpha \cdot I_m^* - (1 - f_c)}. \tag{A18}$$

As in Eq. A9, $[Ca^{2+}]_m$ may be obtained by substituting $I_m^* = I_{tot}^* - I_c^*$ in Eq. A18,

$$[Ca^{2+}]_m = K_d \cdot \frac{\alpha \cdot (I_{tot}^* - I_c^*) - \beta \cdot (1 - f_c)}{(1 - f_c) - \alpha \cdot (I_{tot}^* - I_c^*)}. \tag{A19}$$

The relationship between $[Ca^{2+}]_m$ and $[Ca^{2+}]_c$, at a particular pacing frequency, freq, and diastole is obtained by substituting I_c^* from Eq. A15 into Eq. A19,

$$[Ca^{2+}]_m(\text{freq}) = K_d \cdot \frac{\alpha \cdot I_{tot}^*(\text{freq}) - f_c \cdot I([Ca^{2+}]_c(\text{freq})) - \beta \cdot (1 - f_c)}{(1 - f_c) - \alpha \cdot I_{tot}^*(\text{freq}) + f_c \cdot I([Ca^{2+}]_c(\text{freq}))}, \tag{A20a}$$

where

$$I([Ca^{2+}]_c(\text{freq})) = \frac{[Ca^{2+}]_c(\text{dia, freq}) + \beta \cdot K_d}{[Ca^{2+}]_c(\text{dia, freq}) + K_d}. \tag{A20b}$$

Thus, provided that f_c and $[Ca^{2+}]_c$ can independently be determined, Eq. A20 shows that an estimate of $[Ca^{2+}]_m$ may be obtained even when Rhod-2 partially loads into the cytosol, and estimates of mitochondrial I_{max} and I_{min} are not available.

Rhod-2 measurements of $[Ca^{2+}]_m$(0.25 Hz) (using known $[Ca^{2+}]_c$(dia, 0.25) from Indo-1 measurements)

To determine $[Ca^{2+}]_m$ at 0.25-Hz pacing frequency, Rhod-2-loaded trabeculae are used to determine $I_{tot}^*(0.25)$, while Indo-1-loaded trabeculae are used to determine diastolic $[Ca^{2+}]_c$ at 0.25 Hz. Thus, according to Eq. A20a,

$$[Ca^{2+}]_m(0.25) = K_d \cdot \frac{\alpha \cdot I_{tot}^*(0.25) - f_c \cdot I([Ca^{2+}]_c(0.25)) - \beta \cdot (1 - f_c)}{(1 - f_c) - \alpha \cdot I_{tot}^*(0.25) + f_c \cdot I([Ca^{2+}]_c(0.25))}, \tag{A21}$$

where $I([Ca^{2+}]_c(0.25))$ is given by Eq. A20b with freq = 0.25.

Rhod-2 measurement of $[Ca^{2+}]_m$(2 Hz)

Method 1 (using known $[Ca^{2+}]_c$(dia, 2) from Indo-1 measurements)

$[Ca^{2+}]_m$ may be determined at 2 Hz in a manner analogous to 0.25-Hz pacing frequency,

$$[Ca^{2+}]_m(2) = K_d \cdot \frac{\alpha \cdot I_{tot}^*(2) - f_c \cdot I([Ca^{2+}]_c(2)) - \beta \cdot (1 - f_c)}{(1 - f_c) - \alpha \cdot I_{tot}^*(2) + f_c \cdot I([Ca^{2+}]_c(2))}, \tag{A22}$$

where $I([Ca^{2+}]_c(2))$ is given by Eq. A20b with freq = 2. With this method, $[Ca^{2+}]_m(2)$ depends on Rhod-2 measurements of $I_{tot}^*(2)$ and Indo-1 measurements of $[Ca^{2+}]_c$(dia, 2) in a separate group of trabeculae.

Method 2 (using known $[Ca^{2+}]_c$(dia, 0.25) from Indo-1 measurements)

To determine $[Ca^{2+}]_m(2)$ using $[Ca^{2+}]_c$(dia, 0.25) instead of $[Ca^{2+}]_c$(dia, 2), one may assume differences in the kinetics of $[Ca^{2+}]_c$(dia) versus $[Ca^{2+}]_m$. As shown (see Results), $[Ca^{2+}]_c$(dia) appears to rise much

faster than $[Ca^{2+}]_m$ when the pacing frequency is abruptly increased. Consider the measured intensities (in diastole) obtained at three time points (t_0, t_1, and t_2) as the pacing frequency is increased from 0.25 to 2 Hz (see Fig. 2),

t_0 steady state at 0.25 Hz:

$$I^*_{tot}(0.25) = I^*_c(0.25) + I^*_m(0.25), \quad \text{(A23)}$$

t_1 ~2 s at 2 Hz (init):

$$I^*_{tot}(2_{init}) = I^*_c(2_{init}) + I^*_m(2_{init}), \quad \text{(A24)}$$

t_2 ~180 s at 2 Hz (steady state = SS):

$$I^*_{tot}(2_{SS}) = I^*_c(2_{SS}) + I^*_m(2_{SS}). \quad \text{(A25)}$$

If it is assumed that $[Ca^{2+}]_c$(dia) increases immediately following increased pacing frequency (between t_0 and t_1), while $[Ca^{2+}]_m$ is unchanged, then $I^*_m(2_{init}) = I^*_m(0.25)$. Furthermore, as shown in the Results, $[Ca^{2+}]_c$(dia) is constant after the immediate rise (between t_1 and t_2), and therefore $I^*_c(2_{init}) = I^*_c(2_{SS})$. Substituting these two relationships into Eq. A24 and combining Eqs. A23–A25 gives

$$I^*_m(2_{SS}) = I^*_{tot}(0.25) + I^*_{tot}(2_{SS}) - I^*_{tot}(2_{init}) - I^*_c(0.25). \quad \text{(A26)}$$

Eq. A26 is qualitatively similar to Eq. A2, and $[Ca^{2+}]_m(2)$ can thus again be obtained from Eq. A20 by replacing I^*_{tot}(freq) with $[I^*_{tot}(0.25) + I^*_{tot}(2_{SS}) - I^*_{tot}(2_{init})]$ and $[Ca^{2+}]_c$(dia, freq) with $[Ca^{2+}]_c$(dia, 0.25) (in contrast to using $I^*_{tot}(2)$ and $[Ca^{2+}]_c$(dia, 2) in Method 1):

$$[Ca^{2+}]_m(2) = K_d \cdot \frac{\left\{\begin{array}{r}\alpha \cdot [I^*_{tot}(0.25) + I^*_{tot}(2_{SS}) - I^*_{tot}(2_{init})] \\ -f_c \cdot I([Ca^{2+}]_c(0.25)) - \beta \cdot (1 - f_c)\end{array}\right\}}{\left\{\begin{array}{r}(1 - f_c) - \alpha \cdot [I^*_{tot}(0.25) + I^*_{tot}(2_{SS}) - I^*_{tot}(2_{init})] \\ +f_c \cdot I([Ca^{2+}]_c(0.25))\end{array}\right\}}, \quad \text{(A27)}$$

where $I([Ca^{2+}]_c(0.25))$ is given by Eq. A20b with freq = 0.25.

The disadvantage of Method 2 is that it is based on the assumption that $[Ca^{2+}]_m$ does not initially increase when the pacing frequency is abruptly increased (between t_0 and t_1). If this is not correct, $I^*_m(0.25) < I^*_m(2_{init})$, causing $I^*_m(2_{SS})$ and consequently $[Ca^{2+}]_m(2)$ to be underestimated. Conversely, if $[Ca^{2+}]_m(2)$ is similar, regardless of Method (1 versus 2), this would suggest that $[Ca^{2+}]_m$ does not initially increase when the pacing frequency is abruptly increased.

Rhod-2 measurements of $[Ca^{2+}]_c$(dia, 2) (using known $[Ca^{2+}]_c$(dia, 0.25) from Indo-1 measurements)

Rhod-2 can also be used to measure $[Ca^{2+}]_c$(dia, 2) if $[Ca^{2+}]_c$(dia, 0.25) is independently known (e.g., from Indo-1 measurements). If it is again assumed that $I^*_m(2_{init}) = I^*_m(0.25)$, then subtracting Eq. A24 from Eq. A23 shows that

$$I^*_c(2_{init}) = I^*_{tot}(2_{init}) - I^*_{tot}(0.25) + I^*_c(0.25). \quad \text{(A28)}$$

An expression for $[Ca^{2+}]_c$(dia, 2) is subsequently obtained by substituting $I^*_c(2_{init})$ into Eq. A17,

$$[Ca^{2+}]_c(\text{dia}, 2) = K_d \cdot \frac{f_c \cdot \beta - \alpha \cdot \{I^*_{tot}(2_{init}) - I^*_{tot}(0.25) + I^*_c(0.25)\}}{\alpha \cdot \{I^*_{tot}(2_{init}) - I^*_{tot}(0.25) + I^*_c(0.25)\} - f_c}. \quad \text{(A29)}$$

The relationship between $[Ca^{2+}]_c$(dia, 2) and $[Ca^{2+}]_c$(dia, 0.25) is finally obtained by substituting $I^*_c(0.25)$ using Eq. A15,

$$[Ca^{2+}]_c(\text{dia}, 2) = K_d \cdot \frac{\left\{\begin{array}{r}f_c \cdot [\beta - I([Ca^{2+}]_c(0.25))] \\ -\alpha \cdot [I^*_{tot}(2_{init}) - I^*_{tot}(0.25)]\end{array}\right\}}{\left\{\begin{array}{r}f_c \cdot [I([Ca^{2+}]_c(0.25)) - 1] \\ +\alpha \cdot [I^*_{tot}(2_{init}) - I^*_{tot}(0.25)]\end{array}\right\}}, \quad \text{(A30)}$$

where $I([Ca^{2+}]_c(0.25))$ is given by Eq. A20b with freq = 0.25. $\Delta[Ca^{2+}]_c$(dia) is simply calculated by subtracting $[Ca^{2+}]_c$(dia, 0.25) (separately obtained from Indo-1 measurements) from $[Ca^{2+}]_c$(dia, 2).

The disadvantage of this method is that it is again based on the assumption that $[Ca^{2+}]_m$ does not initially increase when the pacing frequency is abruptly increased (between t_0 and t_1). If this is not correct, $I^*_m(0.25) < I^*_m(2_{init})$, causing $I^*_c(2_{init})$ and consequently $[Ca^{2+}]_c$(dia, 2) to be overestimated. Conversely, if $[Ca^{2+}]_c$(dia, 2) is similar, regardless of dye (Indo-1 versus Rhod-2), this would suggest that $[Ca^{2+}]_m$ does not initially increase when the pacing frequency is abruptly increased.

Approximations

$I_{Mn^{2+}}$ (needed to determine $I^*_{tot}(0.25)$) and f_c were individually measured in each trabecula to calculate $[Ca^{2+}]_m(0.25)$ (Eq. A21). The reported $[Ca^{2+}]_m(0.25)$ is thus an average of the individually measured $[Ca^{2+}]_m(0.25)$ in each trabecula. However, $I_{Mn^{2+}}$ and f_c were not measured in all experiments where the pacing frequency was altered. The average value of f_c (= 47%; see Results) was therefore used in those cases. Furthermore, for each trabecula, the values $I^*_{tot}(2)$, $[I^*_{tot}(0.25) + I^*_{tot}(2_{SS}) - I^*_{tot}(2_{init})]$ (Eq. A26) and $[I^*_{tot}(2_{init}) - I^*_{tot}(0.25)]$ (Eq. A28) were approximated according to

$$I^*_{tot}(2) \sim \frac{I_{tot}(2)}{I_{tot}(0.25)} \cdot I^*_{tot}(0.25), \quad \text{(A31)}$$

$$I^*_{tot}(0.25) + I^*_{tot}(2_{SS}) - I^*_{tot}(2_{init}) \sim \frac{I_{tot}(0.25) + I_{tot}(2_{SS}) - I_{tot}(2_{init})}{I_{tot}(0.25)} \cdot I^*_{tot}(0.25), \quad \text{(A32)}$$

$$I^*_{tot}(2_{init}) - I^*_{tot}(0.25) \sim \frac{I_{tot}(2_{init}) - I_{tot}(0.25)}{I_{tot}(0.25)} \cdot I^*_{tot}(0.25). \quad \text{(A33)}$$

Thus, the first factor in Eqs. A31–A33 were measured in each trabecula, and then multiplied with the average value of $I^*_{tot}(0.25)$ (= 1.33; see Results) to obtain the approximations.

This work was supported by grants from National Institutes of Health Heart, Lung, and Blood Institute HL-57562 (R.B.) and HL-30077 (D.M.B.).

REFERENCES

Ashruf, J. F., J. M. C. C. Coremans, H. A. Bruining, and C. Ince. 1995. Increase of cardiac work is associated with decrease of mitochondrial NADH. *Am. J. Physiol. Heart Circ. Physiol.* 269:H856–H862.

Backx, P. H., and H. E. Ter Keurs. 1993. Fluorescent properties of rat cardiac trabeculae microinjected with fura-2 salt. *Am. J. Physiol. Heart Circ. Physiol.* 264:H1098–H1110.

Baker, A. J., R. Brandes, J. H. Schreur, S. A. Camacho, and M. W. Weiner. 1994. Protein and acidosis alter calcium-binding and fluorescence spectra of the calcium indicator indo-1. *Biophys. J.* 67:1646–1654.

Bassani, J. W., R. A. Bassani, and D. M. Bers. 1993. Ca^{2+} cycling between sarcoplasmic reticulum and mitochondria in rabbit cardiac myocytes. *J. Physiol.* 460:603–621.

Brandes, R. 1999. Restoration of mitochondrial protonmotive force with increased cardiac work is substrate dependent. *Circulation.* 100:198. (abstr.)

Brandes, R., and D. M. Bers. 1996. Increased work in cardiac trabeculae causes decreased mitochondrial NADH fluorescence followed by slow recovery. *Biophys. J.* 71:1024–1035.

Brandes, R., and D. M. Bers. 1997. Intracellular Ca^{2+} increases the mitochondrial NADH concentration during elevated work in intact cardiac muscle. *Circ. Res.* 80:82–87.

Brandes, R., and D. M. Bers. 1999. Analysis of the mechanisms of mitochondrial NADH regulation in cardiac trabeculae. *Biophys. J.* 77: 1666–1682.

Brandes, R., V. M. Figueredo, S. A. Camacho, A. J. Baker, and M. W. Weiner. 1993a. Investigation of factors affecting fluorometric quantitation of cytosolic [Ca^{2+}] in perfused hearts. *Biophys. J.* 65:1983–1993.

Brandes, R., V. M. Figueredo, S. A. Camacho, A. J. Baker, and M. W. Weiner. 1993b. Quantitation of cytosolic [Ca^{2+}] in whole perfused rat hearts using Indo-1 fluorometry. *Biophys. J.* 65:1973–1982.

Brandes, R., V. M. Figueredo, S. A. Camacho, B. M. Massie, and M. W. Weiner. 1992. Suppression of motion artifacts in fluorescence spectroscopy of perfused hearts. *Am. J. Physiol. Heart Circ. Physiol.* 263: H972–H980.

Brandes, R., V. M. Figueredo, S. A. Camacho, and M. W. Weiner. 1994. Compensation for changes in tissue light absorption in fluorometry of hypoxic perfused rat hearts. *Am. J. Physiol. Heart Circ. Physiol.* 266: H2554–H2567.

Brandes, R., L. S. Maier, and D. M. Bers. 1998. Regulation of mitochondrial [NADH] by cytosolic [Ca^{2+}] and work in trabeculae from hypertrophic and normal rat hearts. *Circ. Res.* 82:1189–1198.

Buntinas, L., K. K. Gunter, G. C. Sparagna, and T. E. Gunter. 2001. The rapid mode of calcium uptake into heart mitochondria (RaM): comparison to RaM in liver mitochondria. *Biochim. Biophys. Acta.* 1504: 248–261.

Cox, D. A., and M. A. Matlib. 1993. A role for the mitochondrial Na^+–Ca^{2+} exchanger in the regulation of oxidative phosphorylation in isolated heart mitochondria. *J. Biol. Chem.* 268:938–947.

Crompton, M. 1990. The role of Ca^{2+} in the function and dysfunction of heart mitochondria. *In* Calcium and the Heart. G. A. Langer, editor. Raven Press Ltd., New York. 167–199.

del Nido, P. J., P. Glynn, P. Buenaventura, G. Salama, and A. P. Koretsky. 1998. Fluorescence measurement of calcium transients in perfused rabbit heart using Rhod 2. *Am. J. Physiol. Heart Circ. Physiol.* 274: H728–H741.

Di Lisa, F., G. Gambassi, H. Spurgeon, and R. G. Hansford. 1993. Intramitochondrial free calcium in cardiac myocytes in relation to dehydrogenase activation. *Cardiovasc. Res.* 27:1840–1844.

Eng, J., R. M. Lynch, and R. S. Balaban. 1989. Nicotinamide adenine dinucleotide fluorescence spectroscopy and imaging of isolated cardiac myocytes. *Biophys. J.* 55:621–630.

Griffiths, E. J., H. Lin, and M. S. Suleiman. 1998. NADH fluorescence in isolated guinea-pig and rat cardiomyocytes exposed to low or high stimulation rates and effect of metabolic inhibition with cyanide. *Biochem. Pharmacol.* 56:173–179.

Griffiths, E. J., M. D. Stern, and H. S. Silverman. 1997a. Measurement of mitochondrial calcium in single living cardiomyocytes by selective removal of cytosolic Indo 1. *Am. J. Physiol. Cell Physiol.* 273:C37–C44.

Griffiths, E. J., S. K. Wei, M. P. Haigney, C. J. Ocampo, M. D. Stern, and H. S. Silverman. 1997b. Inhibition of mitochondrial calcium efflux by clonazepam in intact single rat cardiomyocytes and effects on NADH production. *Cell Calcium.* 21:321–329.

Grynkiewicz, G., M. Poenie, and R. Y. Tsien. 1985. A new generation of Ca^{2+} indicators with greatly improved fluorescence properties. *J. Biol. Chem.* 260:3440–3450.

Gunter, T. E., K. K. Gunter, S. S. Sheu, and C. E. Gavin. 1994. Mitochondrial calcium transport: physiological and pathological relevance. *Am. J. Physiol. Cell Physiol.* 267:C313–C339.

Hansford, R. G. 1991. Dehydrogenase activation by Ca^{2+} in cells and tissues. [Review]. *J. Bioenerg. Biomembr.* 23:823–854.

Haworth, R. A., and D. Redon. 1998. Calibration of intracellular Ca transients of isolated adult heart cells labelled with fura-2 by acetoxymethyl ester loading. *Cell Calcium.* 24:263–273.

Hove-Madsen, L., and D. M. Bers. 1992. Indo-1 binding to protein in permeabilized ventricular myocytes alters its spectral and Ca binding properties. *Biophys. J.* 63:89–97.

Hunter, D. R., R. A. Haworth, and H. A. Berkoff. 1981. Cellular manganese uptake by the isolated perfused rat heart: a probe for the sarcolemma calcium channel. *J. Mol. Cell. Cardiol.* 13:823–832.

Hunter, D. R., H. Komai, R. A. Haworth, M. D. Jackson, and H. A. Berkoff. 1980. Comparison of Ca^{2+}, Sr^{2+}, and Mn^{2+} fluxes in mitochondria of the perfused rat heart. *Circ. Res.* 47:721–727.

Jacobus, W. E., R. W. Moreadith, and K. M. Vandegaer. 1982. Mitochondrial respiratory control. Evidence against the regulation of respiration by extramitochondrial phosphorylation potentials or by [ATP]/[ADP] ratios. *J. Biol. Chem.* 257:2397–2402.

Koretsky, A. P., L. A. Katz, and R. S. Balaban. 1987. Determination of pyridine nucleotide fluorescence from the perfused heart using an internal standard. *Am. J. Physiol. Heart Circ. Physiol.* 253:H856–H862.

Leyssens, A., A. V. Nowicky, L. Patterson, M. Crompton, and M. R. Duchen. 1996. The relationship between mitochondrial state, ATP hydrolysis, $[Mg^{2+}]_i$ and $[Ca^{2+}]_i$ studied in isolated rat cardiomyocytes. *J. Physiol. (Lond.).* 496:111–128.

Maier, L. S., R. Brandes, B. Pieske, and D. M. Bers. 1998. Effects of left ventricular hypertrophy on force and Ca^{2+} handling in isolated rat myocardium. *Am. J. Physiol. Heart Circ. Physiol.* 43:H1361–H1370.

McCormack, J. G., A. P. Halestrap, and R. M. Denton. 1990. Role of calcium ions in regulation of mammalian intramitochondrial metabolism. [Review]. *Physiol. Rev.* 70:391–425.

Miyata, H., H. S. Silverman, S. J. Sollott, E. G. Lakatta, M. D. Stern, and R. G. Hansford. 1991. Measurement of mitochondrial free Ca^{2+} concentration in living single rat cardiac myocytes. *Am. J. Physiol. Heart Circ. Physiol.* 261:H1123–H1134.

Nuutinen, E. M. 1984. Subcellular origin of the surface fluorescence of reduced nicotinamide nucleotides in the isolated perfused rat heart. *Basic Res. Cardiol.* 79:49–58.

Schreur, J. H., V. M. Figueredo, M. Miyamae, D. M. Shames, A. J. Baker, and A. C. Camacho. 1996. Cytosolic and mitochondrial [Ca^{2+}] in whole hearts using Indo-1 acetoxymethyl ester: effects of high extracellular Ca^{2+}. *Biophys. J.* 70:2571–2580.

Sparagna, G. C., K. K. Gunter, S. S. Shen, and T. E. Gunter. 1995. Mitochondrial calcium uptake from physiological-type pulses of calcium—a description of the rapid uptake mode. *J. Biol. Chem.* 270: 27510–27515.

Spurgeon, H. A., M. D. Stern, G. Baartz, S. Raffaeli, R. G. Hansford, A. Talo, E. G. Lakatta, and M. C. Capogrossi. 1990. Simultaneous measurement of Ca^{2+}, contraction, and potential in cardiac myocytes. *Am. J. Physiol. Heart Circ. Physiol.* 258:H574–H586.

Territo, P. R., S. A. French, M. C. Dunleavy, F. J. Evans, and R. S. Balaban. 2001. Calcium activation of heart mitochondrial oxidative phosphorylation: rapid kinetics of mVO2, NADH, and light scattering. *J. Biol. Chem.* 276:2586–2599.

Territo, P. R., V. K. Mootha, S. A. French, and R. S. Balaban. 2000. Ca^{2+} activation of heart mitochondrial oxidative phosphorylation: role of the *F*(0)/*F*(1)–ATPase. *Am. J. Physiol. Cell Physiol.* 278:C423–C435.

Trollinger, D. R., W. E. Cascio, and J. J. Lemasters. 2000. Mitochondrial calcium transients in adult rabbit cardiac myocytes: inhibition by ruthenium red and artifacts caused by lysosomal loading of Ca^{2+}-indicating fluorophores. *Biophys. J.* 79:39–50.

Unitt, J. F., J. G. McCormack, D. Reid, L. K. MacLachlan, and P. J. England. 1989. Direct evidence for a role of intramitochondrial Ca^{2+} in the regulation of oxidative phosphorylation in the stimulated rat heart. Studies using ^{31}P n.m.r. and ruthenium red. *Biochem. J.* 262:293–301.

Wan, B., C. Doumen, J. Duszynski, G. Salama, T. C. Vary, and K. F. La Noue. 1993. Effects of cardiac work on electrical potential gradient across mitochondrial membrane in perfused rat hearts. *Am. J. Physiol. Heart Circ. Physiol.* 265:H453–H460.

White, R. L., and B. A. Wittenberg. 1995. Effects of calcium on mitochondrial NAD(P)H in paced rat ventricular myocytes. *Biophys. J.* 69:2790–2799.